



Combining hyper-resolution land surface modeling with SMAP brightness temperatures to obtain 30-m soil moisture estimates

Noemi Vergopolan^{a,*}, Nathaniel W. Chaney^b, Hylke E. Beck^a, Ming Pan^a, Justin Sheffield^c, Steven Chan^d, Eric F. Wood^a

^a Department of Civil and Environmental Engineering, Princeton University, United States of America

^b Department of Civil and Environmental Engineering, Duke University, United States of America

^c School of Geography and Environmental Science, Southampton University, United Kingdom

^d NASA Jet Propulsion Laboratory, California Institute of Technology, United States of America



ARTICLE INFO

Edited by Jing M. Chen

Keywords:

Land surface modeling
Data merging
Soil moisture
Brightness temperature
Hyper-resolution
Field-scale
SMAP

ABSTRACT

Accurate and detailed soil moisture information is essential for, among other things, irrigation, drought and flood prediction, water resources management, and field-scale (i.e., tens of m) decision making. Recent satellite missions measuring soil moisture from space continue to improve the availability of soil moisture information. However, the utility of these satellite products is limited by the large footprint of the microwave sensors. This study presents a merging framework that combines a hyper-resolution land surface model (LSM), a radiative transfer model (RTM), and a Bayesian scheme to merge and downscale coarse resolution remotely sensed hydrological variables to a 30-m spatial resolution. The framework is based on HydroBlocks, an LSM that solves the field-scale spatial heterogeneity of land surface processes through interacting hydrologic response units (HRUs). The framework was demonstrated for soil moisture by coupling HydroBlocks with the Tau-Omega RTM used in the Soil Moisture Active Passive (SMAP) mission. The brightness temperature from the HydroBlocks-RTM and SMAP L3 were merged to obtain updated 30-m soil moisture. We validated the downscaled soil moisture estimates at four experimental watersheds with dense in-situ soil moisture networks in the United States and obtained overall high correlations (> 0.81) and good mean KGE score (0.56). The downscaled product captures the spatial and temporal soil moisture dynamics better than SMAP L3 and L4 product alone at both field and watershed scales. Our results highlight the value of hyper-resolution modeling to bridge the gap between coarse-scale satellite retrievals and field-scale hydrological applications.

1. Introduction

Monitoring and forecasting of hydrological, biophysical, and ecological processes at scales that are relevant for decision making is critical for water management. For instance, soil moisture, surface temperature, evapotranspiration, snow water equivalent, irrigation water demands, crop yields, droughts, floods, erosion risk, epidemic disease outbreaks, and ecosystem services are states and processes highly linked to the fine-scale interactions between water, energy, and carbon fluxes at the land surface (Koster and Suarez, 1992; Wood et al., 2011; Crow et al., 2012). While in-situ measurements are often sparse and expensive, visible-infrared and microwave-based satellite retrievals offer a unique opportunity for global and continental monitoring of soil moisture, surface temperature, and evapotranspiration (Pan and Wood, 2010). There is, however, a critical gap between the coarse spatial scale

of space-born remotely sensed retrievals and field-scale applications. This scale gap is an issue as fine-scale hydrological interactions play a key role in the spatial-temporal dynamics of hydrological and biophysical processes. Consequently, the failure to represent landscape heterogeneity in hydrological estimates leads to deficiencies in representing the fluxes and feedbacks of the water, energy, and carbon cycles (Pachepsky et al., 2003; Falloon et al., 2011; Piles et al., 2011; Chaney et al., 2018).

To overcome the spatial scale gap between satellite retrievals and water management applications, spatial downscaling techniques have been developed that use geostatistics, machine learning, land surface models (LSMs), and data assimilation (for reviews, see Reichle, 2008; Srivastava et al., 2013; Atkinson, 2013; Peng et al., 2017). Statistical and machine learning methods have been applied to downscale coarse-scale satellite retrievals based on high-resolution remotely sensed

* Corresponding author at: 59 Olden St., EQUAD CEE E209, Princeton, NJ 08544, United States of America.
E-mail address: noemi@princeton.edu (N. Vergopolan).

proxies. For instance, DisALEXI disaggregates GOES 5-km surface flux estimates to 10–100 m by using high spatial resolution radiative and optical remotely sensed proxies, such as a vegetation index and surface temperature from ASTER, Landsat, and MODIS (Norman et al., 2003). More recently, for soil moisture, Sadeghi et al. (2017) proposed an optical trapezoid model based on the distribution of land surface temperature and vegetation in Sentinel-2 and Landsat-8 to derive the physical relation between soil moisture and shortwave infrared reflectance. Fang et al. (2019) proposed a more data-intensive approach that uses a change detection disaggregation algorithm to combine PALS observations (Passive and Active L-band system) at 1600-m with radar backscatter from an Unmanned Air Vehicle Synthetic Aperture Radar (UAVSAR) to estimate soil moisture at 5–800 m. Ojha et al. (2019) proposed a stepwise disaggregation of SMAP to 100-m resolution using 1-km MODIS land surface temperature and NDVI and Landsat-7/8 land surface temperature. Although downscaling using statistical and machine learning approaches are trained on high-resolution remotely sensed data proxies, they often do not consider the interactions of the landscape with current meteorological conditions and thus do not resolve the physical processes (Peng et al., 2017). This leads to statistical relationships that can be satisfied locally but potentially not regionally, resulting in models that are prone to overfitting and are often do not generalize well (Liu et al., 2017). In addition, inference from high-resolution optical sensors (visible and near-infrared thermal) is affected by atmospheric attenuation and dense vegetation (Bindlish et al., 2003; de Jeu et al., 2008; Jones et al., 2011), and it is subject to the coarse temporal resolution of their retrieved products.

A well-established methodology to address the lack of physical process interpretability and model transferability is to combine radiative transfer models (RTMs) and land surface models (LSMs). RTMs use satellite-based radiative temperature observations and ancillary information on soil properties, vegetation, and meteorological conditions to model hydrological processes (Jackson, 1993; Njoku and Li, 1999; Drusch et al., 2005). LSMs are physically-based models that simulate hydrological processes, dynamically accounting for the water and energy balances, and sometimes also accounting for the carbon cycle, vegetation dynamics, and groundwater flows. More recently, LSMs have also accounted for human activities such as irrigation, groundwater, and surface water abstractions, and reservoir operations (Bierkens et al., 2015). The main advantage of combining LSMs and RTMs is the ability to estimate radiative variables and merge them with the satellite observations. This strategy has been widely used to assimilate land surface variables such as SMAP and SMOS soil moisture (Crow and Van Loon, 2006; Pan et al., 2014; De Lannoy and Reichle, 2016a; Lievens et al., 2016), with more recently the SMAP-L4 using dynamic data assimilation to lead this effort (Reichle et al., 2017; Reichle et al., 2018a). Land surface models have also been used to directly assimilate surface temperature (Reichle et al., 2010; Ghent et al., 2010) and snow water equivalent (Andreadis and Lettenmaier, 2006; Clark et al., 2006; Huang et al., 2008; De Lannoy et al., 2012; Durand and Margulis, 2006; Painter et al., 2016).

Although RTMs offer unique opportunities, their accuracy is limited by the significant uncertainties in the radiative observations themselves, in the coarse-scale ancillary data, and in the spatial scale mismatch during the calibration process (between the coarse-scale grid of the sensor and the point-scale in-situ observations). In addition, most LSMs a) still operate at relatively coarse spatial scales (> 5 km); b) do not account for the sub-grid spatial heterogeneity in soil parameters, vegetation, and topography; or c) neglect fine-scale water, energy, and carbon interactions. Remotely sensed variables, such as brightness temperature, surface emissivity, and vegetation indexes are highly sensitive to the landscape heterogeneity in terms of surface temperature, vegetation, soil moisture, and soil properties (Bindlish et al., 2003; de Jeu et al., 2008; Mironov et al., 2009). Consequently, the homogeneous and coarse-scale representation of hydrological parameters and land surface processes limits the value of traditional coarse-scale LSMs

to merge and downscale satellite observations to field scales.

For satellite observations and models to be truly useful for water management applications, there is a critical need to combine the emerging capability of high-resolution modeling with available fine-scale physiographic data and remote sensing retrievals (Wood et al., 2011). The land surface modeling community is already taking advantage of big data analytics, high-performance computing, and hyper-resolution modeling to revolutionize hydrological simulations (Wood et al., 2011; Bierkens et al., 2015). HydroBlocks, for example, is a state-of-the-art physically-based hyper-resolution LSM that considers high-resolution ancillary datasets (30–100 m resolution) as drivers of landscape spatial heterogeneity (Chaney et al., 2016). To this end, HydroBlocks clusters areas of similar hydrological behavior into hydrologic response units (HRUs), allowing the model to efficiently simulate hydrological, geophysical, and biophysical processes at an effective 30-m resolution for continental domains.

In this study, we introduce a framework that uses hyper-resolution LSM and RTM to downscale remotely sensed hydrological and biogeophysical variables to an unprecedented 30-m spatial resolution. We demonstrate this framework by merging model and remotely sensed brightness temperature observations for fine-scale soil moisture retrieval. More specifically, the proposed framework couples the HydroBlocks LSM to a Tau-Omega brightness temperature RTM to estimate brightness temperature at fine scales; it uses Bayesian merging to combine these fine-scale estimates with the 36-km Soil Moisture Active Passive (SMAP) brightness temperatures observations. We subsequently retrieve 30-m SMAP-based soil moisture from the merged brightness temperature via the inverse RTM. Although implemented for soil moisture, this physically-based framework also allows for the downscaling of surface temperature as well as snow water equivalent to 30-m spatial resolution, and it can also be adapted for evapotranspiration and crop water requirements estimates. The proposed merging and downscaling framework is described in Section 2.3. The results are evaluated at four densely monitored experimental watersheds in the United States: Little River (GA), Little Washita (OK), Reynolds Creek (ID), and Walnut Gulch (AZ). The performance of the downscaled soil moisture (as well as the SMAP L3 and the SMAP L4 products) is assessed using in-situ observations. In addition, we perform an uncertainty analysis of the Bayesian merging scheme. This work aims to inform the scientific community on (i) how hyper-resolution land surface modeling can aid the assimilation of remotely sensed observations and improve the representation of landscape heterogeneity; and (ii) the reliability of the merged brightness temperature in providing relevant soil moisture information for scientific and water management applications.

2. Data and methods

Despite the significant implications for soil moisture data for hydrological studies and water management, in-situ observations are costly and sparse. Microwave-based satellite remote sensing offers unique opportunities for large-scale monitoring, but with the limitation of the coarse spatial resolution. Given these challenges, we demonstrated the potential for using hyper-resolution land surface modeling to merge and downscale remotely sensed observations. In the next sections, we present details in the implementation of the HydroBlocks LSM, the Tau-Omega RTM, the Bayesian merging, and the SMAP-based 30-m soil moisture retrieval.

2.1. Hydrological modeling

2.1.1. HydroBlocks land surface model

HydroBlocks is a field-scale resolving land surface model (Chaney et al., 2016) that accounts for the water, energy, and carbon balance to solve land surface processes at an effective hourly, 30-m resolution. HydroBlocks leverages the repeating patterns that exist over the

landscape (i.e., the spatial organization) by clustering areas of assumed similar hydrologic behavior into HRUs. The simulation of these HRUs and their spatial interactions allows the modeling of hydrological, geophysical, and biophysical processes at the field-scale (30 m) over regional to continental extents (Chaney et al., 2016). The core of HydroBlocks is the Noah-MP (Niu et al., 2011) vertical land surface scheme. HydroBlocks applies Noah-MP in an HRU framework to explicitly represent the spatial heterogeneity of surface processes down to field scale. At each time step, the land surface scheme updates the hydrological states at each HRU; and the HRUs dynamically interact laterally via subsurface flow.

To enable a realistic representation of horizontal exchanges while preserving the high computational efficiency of HRUs, HydroBlocks implements a multi-scale hierarchical clustering (HRU generation) scheme that operates at several critical spatial scales identified for the underlying hydrological, geophysical and biophysical processes (Chaney et al., 2018):

- (a) *Catchments*: defined by topography and serve as the boundary for surface flows;
- (b) *Characteristics hillslopes*: defined by topography and environmental similarity;
- (c) *Height bands*: defined by the height above nearest drainage (HAND) and define the primary flow directions and temperature gradient;
- (d) *Tiles (HRUs)*: defined by multiple soil/vegetation/land cover characteristics and serve as the smallest modeling units.

With this hierarchical setup, HydroBlocks handles mass/energy exchanges within a modeling unit (at a certain scale) separately from the exchanges across the units at that scale. This enables full and realistic horizontal coupling while ensuring computational efficiency.

2.1.2. Hydrological modeling experiment

In this study, the HydroBlocks LSM was used to simulate the land surface processes at 30-m, 1-h resolution from 2010 to 2017 using 500 HRUs per watershed. The meteorological inputs to the model consist of 3-km (1/32°), 1-h meteorological forcing from the Princeton CONUS Forcing (PCF) dataset (Pan et al., 2016) which was developed by downscaling North American Land Data Assimilation System 2 (NLDAS-2) data in combination with several higher resolution products. The precipitation combines the Stage IV and Stage II radar/gauge products with NLDAS-2, the shortwave radiation combines GOES Surface and Insolation Product (GSIP) with NLDAS-2, while the other field variables are downscaled from NLDAS-2. An elevation-based downscaling/fusion procedure is used to ensure physical consistency and mass/energy balance. We used the 30-m DEM from the Shuttle Radar Topography Mission (STRM; Farr et al., 2007) and post-processed it to remove pits and derived slope, aspect, topographic index, flow direction, and flow accumulation values. We used the 2016 30-m land cover type from the National Land Cover Database (NLCD; Homer et al., 2015). The soil-water hydraulic parameters used in NOAH-MP were from the 30-m Probabilistic Remapping of SSURGO (POLARIS) dataset (Chaney et al., 2019). We also include 30-m Landsat-derived NDVI for 2010 (USGS; Roy et al., 2010); 30-m Landsat-derived fractions of bare soil and tree cover (USGS; Hansen et al., 2013); and a 500-m MODIS-derived irrigated-land map (Global Rainfed, Irrigated and Paddy Croplands - GRIPC; Salmon et al., 2015) as additional high-resolution drivers of landscape heterogeneity for the HRU clustering.

No model calibration was performed in this study to ensure that the validation of the soil moisture products is independent of any direct observation. For the RTM, we used the top 5-cm soil moisture and soil temperature estimates from HydroBlocks for the period between 2015 and 2017, with 2010–2014 used for model spin-up. The clay content from POLARIS, as a by-product of the HRU clustering, was also used as fine-scale input to the emissivity module in the RTM.

2.2. Brightness temperature observations and radiative transfer modeling

2.2.1. Remote sensing observations and retrievals: soil moisture active-passive mission

We used version 5 of the SMAP L3 Radiometer Global Daily 36-km EASE-Grid Soil Moisture product (O'Neill et al., 2018). This product provides L-band brightness temperature observations, the associated soil moisture retrievals, and the RTM ancillary data on a global, cylindrical 36-km Equal-Area Scalable Earth (EASE) grid. The SMAP brightness temperature observations we used in the merging, the soil moisture retrievals were used in the evaluation of the results, and the ancillary data was used to support the RTM modeling. We use the vertical polarization of the SMAP L-band brightness temperature observations for the merging because it tends to offer the best sensitivity to soil moisture retrieval at the top 5 cm of the soil (e.g., Jackson, 1993; Njoku and Li, 1999; O'Neill et al., 2018). In this study, we use only the vertically polarized brightness temperature already corrected and flagged for the quality of the retrievals, i.e. for presence of transient water, frozen ground, snow coverage, and flooding, and as well as steeply sloped topography, or for urban, heavily forested, or permanent snow/ice areas are in effect (O'Neill et al., 2018). The ancillary data of SMAP-L3, that is used in the Tau-Omega RTM in this study, comes primarily from the NASA Goddard Space Flight Center - Global Modeling and Assimilation Office (GMAO) GEOS-5 model (surface temperatures) and other satellite sensors such as MODIS (NDVI, land cover classes, open water fraction, permanent snow/ice, etc.). This data product spans from 31 March 2015 to near present, with measurements at 6:00 am and 6:00 pm passing time and 3–5 days between overpasses.

2.2.2. Radiative transfer model: SMAP tau-omega RTM for brightness temperature

Satellite data products use RTMs and ancillary data to relate the sensor's radiative measurements to physical variables, such as land surface temperature, soil moisture, and evapotranspiration (Karthikeyan et al., 2017). In this work, we refer to a "forward" RTM, or simply RTM, when the radiative temperature measured in space is estimated from the land surface condition and ancillary data. Conversely, we refer to the associated "inverse" RTM when land surface conditions are estimated from observed radiative variables and ancillary data. In general, each satellite may use a different RTM that was designed and calibrated to estimate a given land surface variable.

The SMAP mission uses a Tau-Omega RTM to retrieve soil moisture from surface brightness temperature (T_B , K) observations. SMAP retrievals can capture the soil moisture dynamics because its L-band sensor is able to measure the surface emissivity due to the contrast in dielectric properties between wet and dry soils (Entekhabi et al., 2014; Chan et al., 2016). In the Tau-Omega RTM, the brightness temperature is calculated as the sum of the canopy attenuated soil emission, the direct vegetation emission, and the vegetation emission reflected by the soil and attenuated by the canopy:

$$T_B = \varepsilon_{soil} T_{soil} e^{-\tau/\cos \alpha} + (1 - \omega) T_{veg} (1 - e^{-\tau/\cos \alpha}) \\ + (1 - \varepsilon_{soil})(1 - \omega) T_{veg} (1 - e^{-\tau/\cos \alpha}) e^{-\tau/\cos \alpha} \quad (1)$$

where ε_{soil} is the soil emissivity, ω is the single-scattering albedo within the canopy, τ is the optical depth of the canopy, α is the look angle from nadir, T_{soil} is the soil temperature, and T_{veg} is the vegetation temperature. In this Tau-Omega RTM, the soil emissivity is estimated based on the soil moisture and clay content using the Mironov soil dielectric model (Mironov et al., 2009). Here, for simplicity, a single surface temperature was used to represent the average of the vegetation and surface temperatures. The technical details on the SMAP algorithm and the ancillary data processing can be found in the SMAP Handbook (Entekhabi et al., 2014) and product Algorithm Theoretical Basis Documents (O'Neill et al., 2014, 2018).

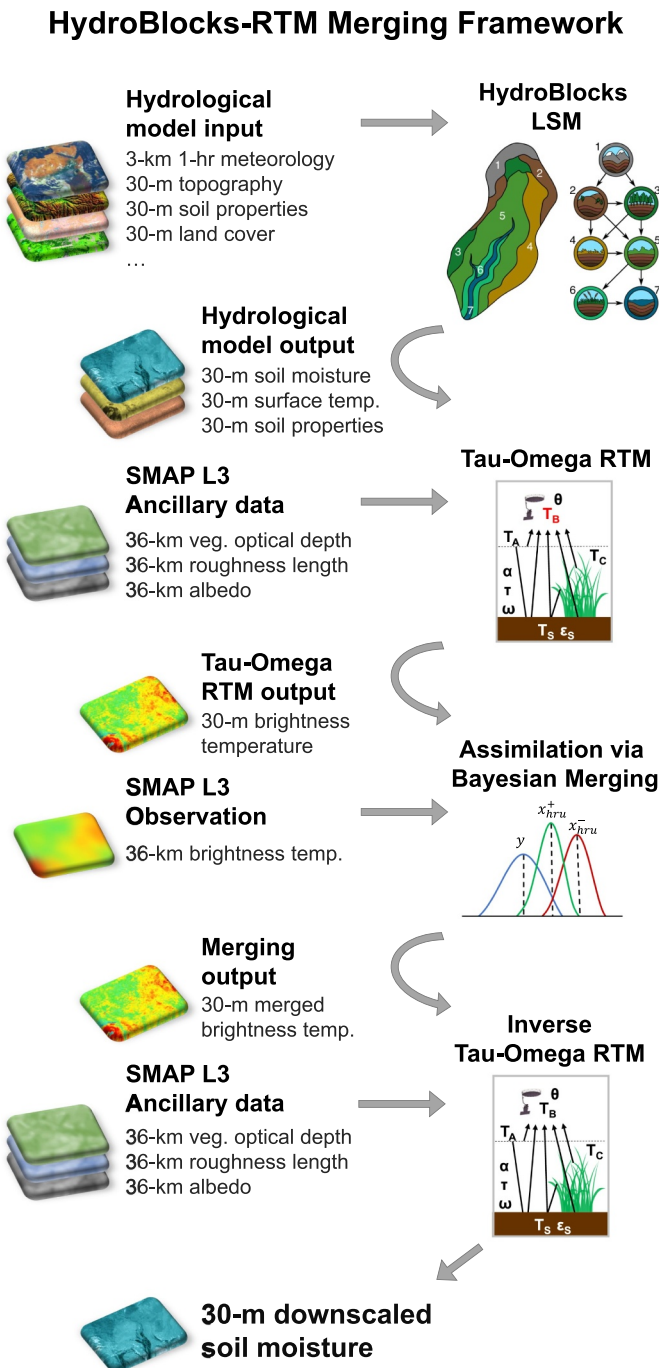


Fig. 1. Flow diagram illustrating the HydroBlocks-RTM merging framework. This framework is applied to merge the 36-km SMAP L3 observed brightness temperature and subsequently retrieve the downscaled soil moisture. It uses the HydroBlocks land surface model, the Tau-Omega radiative transfer model, and Bayesian merging in the HRU-space to obtain 30-m soil moisture estimates.

2.3. Bayesian merging and downscaling framework

The merging and downscaling scheme proposed in this work relies on a three-step process. First, we coupled HydroBlocks and the Tau-Omega RTM to predict brightness temperature at the same fine-scale of HydroBlocks. Then we use Bayes' Theory to merge these fine-scale brightness temperature estimates with the coarse-scale SMAP brightness temperature observations. In the end, once the brightness temperature observations are merged, the inverse RTM is used to retrieve the downscaled soil moisture. Fig. 1 summarizes the workflow for the

brightness temperature merging and the retrieval of the downscaled soil moisture.

Specifically, HydroBlocks LSM was used to estimate hourly top 5-cm soil moisture and soil temperature, as well as clay content from POLARIS — averaged at the HRU — as a by-product of the HydroBlocks clustering analysis. We used the SMAP L3 surface temperature to bias correct HydroBlocks surface temperature prior to the brightness temperature estimation at fine-scale (not included in Fig. 1). This was an optional step that was adopted to reduce the systematic difference between SMAP observed and HydroBlocks-RTM estimated brightness temperatures. And although bias correcting the surface temperature a priori neglects the connectivity between HydroBlocks soil moisture and the new surface temperature, the merging is only performed considering the brightness temperature. Also, the performance of the downscaled soil moisture was found to be superior with this surface temperature bias correction.

As a first step, we estimated the brightness temperature using the HydroBlocks-RTM framework. For input data to the RTM, we used the top 5-cm soil moisture and clay content from HydroBlocks; the 30-m bias-corrected surface temperature; and the 36-km vegetation optical depth, roughness length, and albedo from SMAP-L3 ancillary data. For simplification, we assumed that the above-mentioned 36-km SMAP ancillary data is homogeneously distributed within the SMAP 36-km grid cell. By ensuring consistency with SMAP L3 ancillary data, we leave the differences in the model and the observed brightness temperatures to differences in mostly soil moisture. This helps to isolate the soil moisture signal from the ancillary data. In the second step, we merge the 30-m HydroBlocks-RTM brightness temperature with the 36-km coarse-scale SMAP brightness temperature observations using Bayesian merging (details in the sequence). Once merging was completed, the last step relied on applying the 30-m merged brightness temperature, along with the above-mentioned ancillary data, as inputs into the inverse Tau-Omega RTM to retrieve the final downscaled soil moisture.

The primary motivation for this three-step scheme (RTM, Bayesian merging, and inverse RTM) was to isolate the non-linear relationship between soil moisture and brightness temperature from the merging process. This three-step approach was particularly helpful as (i) Gaussian-based merging and assimilation techniques, such as Bayesian merging, require linearity between the assimilated variables for optimality, and (ii) it allowed us to merge the observed SMAP brightness temperature directly, instead of solely merging the SMAP soil moisture retrieval product on HydroBlocks soil moisture estimates.

2.4. Bayesian merging of brightness temperature

Bayes' Theory was used to merge the HydroBlocks-RTM and SMAP brightness temperatures given its ability to obtain more reliable estimates from noisy observations or estimates. Similar to proposed by Zhan et al. (2006), our merging approach follows a Kalman filter-based scheme but with the merging performed entirely in the HydroBlocks' HRU-space (instead of regular grids) and with each time being merged independently. Fig. 2 illustrates the merging workflow. In this context, the optimal brightness temperature x_t^+ for all the HRUs in the domain at time t can be derived from the fine-scale HydroBlocks-RTM brightness temperature forecast x_t^- (model forecast), updated according to the state update equation:

$$x_t^+ = x_t^- + K [y_t - H x_t^-] \quad (2)$$

In this system, x_t^+ and x_t^- have dimensions $nhru \times 1$, where $nhru$ is the total number of HRUs in the domain. y_t is the vector containing the 36-km SMAP brightness temperature observations at time t . y_t has dimensions $ns \times 1$, where ns is the total number of SMAP grids in the domain. H is the observation operator that maps HydroBlocks-RTM brightness temperatures (x_t^-) from the HRUs scale to the SMAP grid

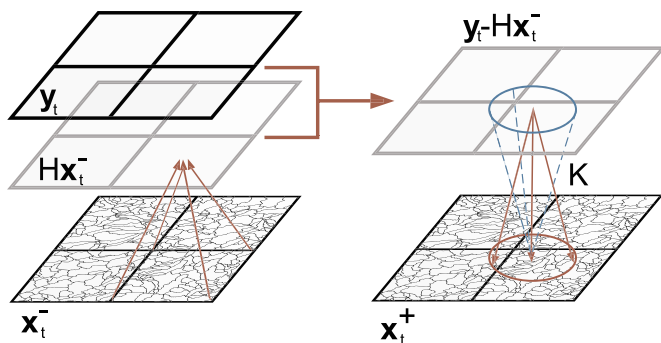


Fig. 2. The proposed approach uses Bayesian merging to combine the HydroBlocks-RTM fine-scale brightness temperature estimates (x_t^-) with the 36-km SMAP observed brightness temperature (y_t) to obtain the optimal brightness temperature estimate (x_t^+). In this work, the merging is performed in the HRU-space, instead of regular grids.

scale. H has dimensions $ns \times nhru$, and it uses a Gaussian-shaped weighted area to account for the relative contribution of each HRU to each SMAP grid. Since the merging is performed using model and observed brightness temperatures, H is in practice a linear Gaussian scaler. Thus, Hx_t^+ is the estimate of HydroBlocks-RTM brightness temperature at the observation scale and it has dimensions $ns \times 1$. The difference in brightness temperature between the SMAP observation and HydroBlocks-RTM forecast in the observation space ($y_t - Hx_t^+$) is herein called the innovation term. K is the gain, and it is calculated based on the relative magnitude between the model and the observation uncertainties:

$$K = \frac{PH^T}{HPH^T + R} \quad (3)$$

In this merging framework, K operates in the HRU-space and it has dimensions $nhru \times ns$. In Eq. (3), R is the observation error covariance matrix and P is the forecast error covariance matrix. The observation error covariance matrix has its diagonal elements set to the SMAP radiometer uncertainty of 1.3 K (Piepmeier et al., 2017), with the off-diagonal set to zero assuming the SMAP observation errors were uncorrelated with each other. The R matrix has dimensions $ns \times ns$. To estimate the errors in the brightness temperature forecast, we consider the model uncertainty and the brightness temperature sensitivity. HydroBlocks has a soil moisture RMSE of approximately $0.05 \text{ m}^3/\text{m}^3$, and based on the brightness temperature sensitivity of 1 K per 0.01 volumetric soil moisture for X band (SMAP handbook; Entekhabi et al., 2014), we estimate the error in the brightness temperature forecast to be around 5^2 K^2 . The P forecast error covariance matrix has dimensions $nhru \times nhru$. We assume that HRUs belonging to the same SMAP grid have correlated errors. Conversely, if an HRU pair belongs to different SMAP grids, the errors are assumed to be uncorrelated. Thus, in the P matrix the entries of correlated HRU pairs were set to 5^2 K^2 , and the entries of uncorrelated HRU pairs were set to zero.

When Eq. (2) is applied to dynamic systems, with both system states and error covariances are updated sequentially, the approach is called the Kalman filter. However, in our study, the merging is performed at each time step independently, and the system states and error covariances are not updated sequentially. In this case, as highlighted by Zhan et al. (2006), Eq. (2) is an implementation of Bayes' Theory.

In our results, we often observed a systematic bias between HydroBlocks and SMAP soil moisture, as well as a bias between HydroBlocks-RTM and SMAP brightness temperatures. This bias between forecast and observed brightness temperature is called the *forecast bias* hereafter. Gaussian-based merging approaches are only optimal when there is no forecast bias between the variables and when both variables have Gaussian-distributed errors that are independent and uncorrelated (Anderson and Moore, 2005). And, consequently, this

forecast bias leads to non-optimal estimates. A common procedure is to remove the forecast bias before the merging, as it showed to improve the optimality of radiative variables assimilation (Reichle et al., 2004; De Lannoy et al., 2007; Kumar et al., 2012; De Lannoy and Reichle, 2016b). We calculated the forecast bias seasonally, using a 3 hourly 4-month window moving average. The 4-month window was identified by testing windows of sizes from 1 to 12 months, and the 4-month window showed the best performance. Once estimated the forecast bias, the merging is performed as follows:

$$x_t^+ = x_t^- + K [(y_t - Hx_t^-) - bias_{forecast}] \quad (4)$$

Similar data merging approaches have been applied previously at spatial resolutions up to 1-km using land surface models and dynamic assimilation for SMAP, SMOS, and AMSR-E (Zhan et al., 2006; Durand and Margulis, 2006; Sahoo et al., 2013; Pan et al., 2014; De Lannoy and Reichle, 2016a, 2016b; Lievens et al., 2016; Lievens et al., 2017). This study builds on these previous efforts to enable hydrological estimates at 30-m spatial resolution. Here, the HRU concept used in HydroBlocks is leveraged to perform both the land surface modeling and the data merging in the HRU space. This implies considering the irregular spatial distribution and contribution of each of the HRU and its surroundings when merging the brightness temperatures. While more complex, working in the HRU space reduces the dimensionality of the system. For instance, one SMAP grid of 36-km by 36-km contains ~ 1.44 million 30-m grid cells. By implementing the HRU-based merging, we reduce the dimension of the system by at least two orders of magnitude, with a resulting $\sim 1500\text{--}2000$ HRUs per SMAP grid. In this way, HRUs allow for highly efficient distributed computing, and it lowers the computational and data storage requirements in comparison to fully distributed setups.

2.5. Evaluation and sensitivity analysis

2.5.1. Framework evaluation

To assess the process representativeness and consistency of the hyper-resolution-derived soil moisture estimates, we evaluated the soil moisture products against in-situ soil moisture observations. The four sites evaluated in this study were Little River (GA), Little Washita (OK), Reynolds Creek (ID), and Walnut Gulch (AZ) experimental watersheds (Fig. 3). These sites were chosen because of their dense in-situ soil moisture networks and their diversity in terms of climate, topography, and vegetation. We used a total of 60 probes from the SMAPVEX15 (<https://smap.jpl.nasa.gov/science/validation/fieldcampaigns/SMAPVEX15/>) and SMAPVEX16 (Colliander et al., 2017, 2019) campaigns.

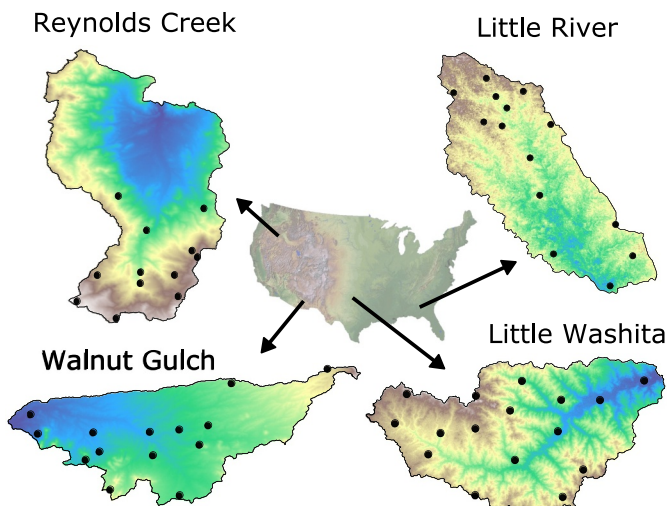


Fig. 3. The four experimental watersheds in which we evaluate the downscaled soil moisture estimates. The black points represent in-situ soil moisture probes.

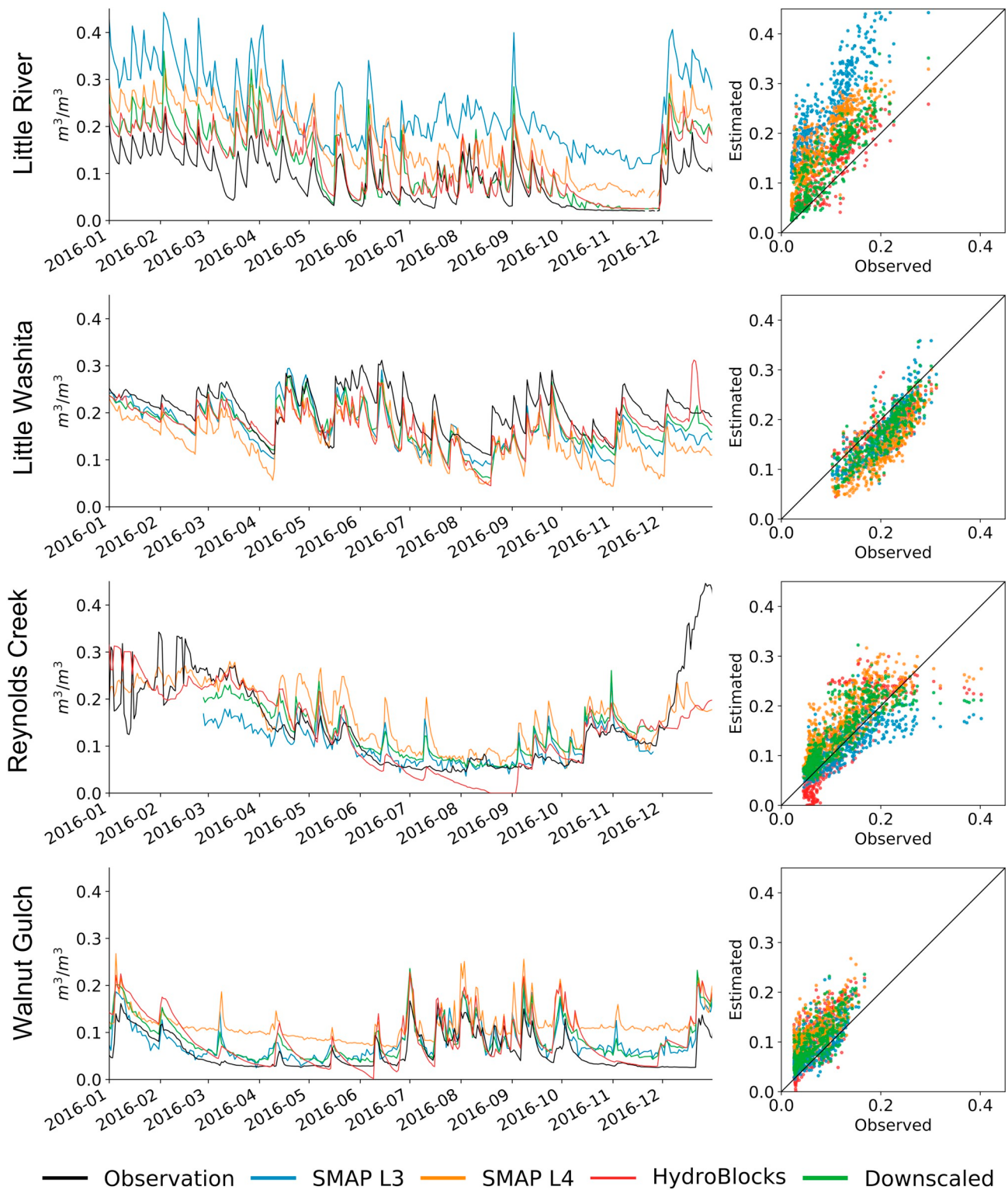


Fig. 4. Time series of daily soil moisture averaged at the in-situ observational network and compared with the basin averaged collocated grid cells. The black line shows the soil moisture as observed by the in-situ probes; the red line shows the HydroBlocks LSM top 5-cm soil moisture; the orange line shows the SMAP L4 soil moisture; the blue line shows the SMAP-L3 soil moisture and the green line the downscaled soil moisture as a result of merging HydroBlocks and SMAP L3 brightness temperatures. The right panel shows the respective scatter plots, which summarize the distribution of all records of each product in comparison to the observations for each evaluation site.

In addition, we compared the performance of our results with the state-of-the-art SMAP L4 Global 3-hourly 9 km EASE-Grid Surface Soil Moisture Analysis Update product (Reichle et al., 2018a). The SMAP-L4 product is computed by using a dynamic assimilating the SMAP

brightness temperatures into the NASA Catchment land surface model (Koster et al., 2000) using a customized version of the Goddard Earth Observing System (GEOS) land data assimilation system (Reichle et al., 2014; Reichle et al., 2018b).

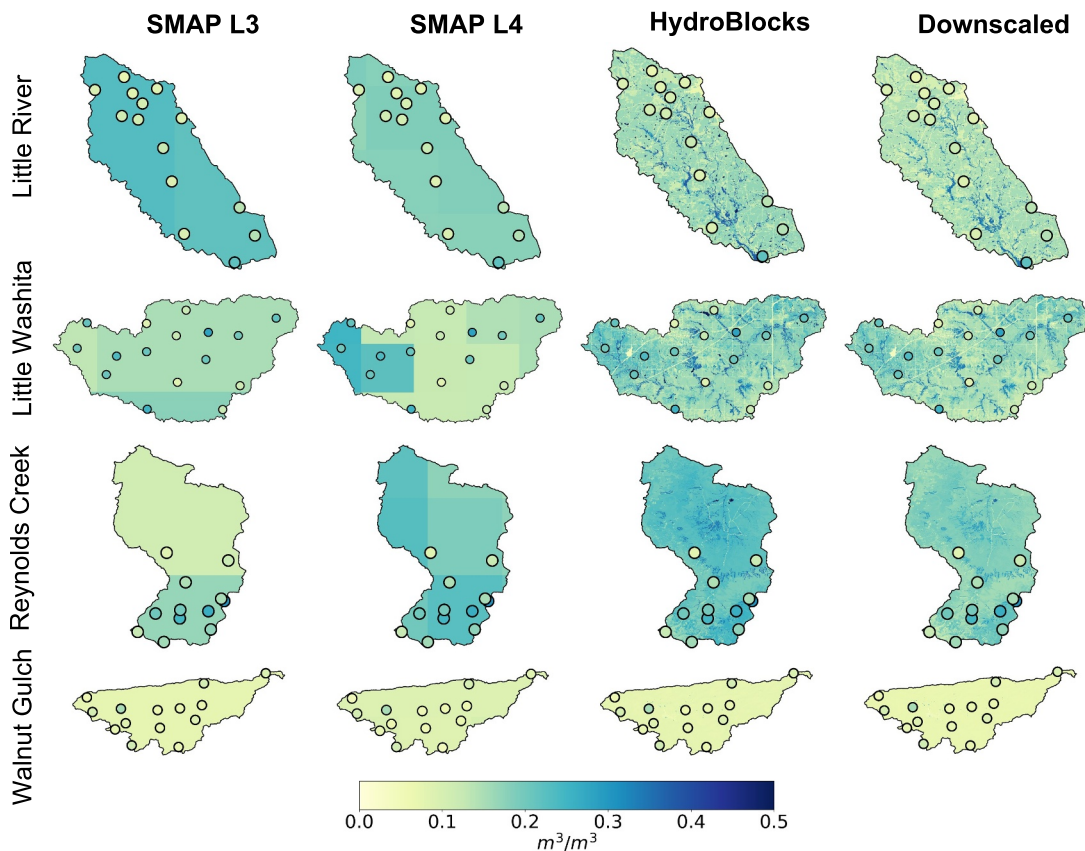


Fig. 5. Mean annual soil moisture of the SMAP L3 product (first column); the SMAP L4 product (second column); the HydroBlocks LSM (third column); the downscaled product via the Bayesian merging (fourth column); and the in-situ observations network (overlaid points) at each of the four evaluation sites (lines).

We compared the in-situ observations with the collocated grid cell of the 36-km SMAP L3 soil moisture, 9-km SMAP L4 soil moisture, 30-m HydroBlocks soil moisture, and 30-m downscaled soil moisture, at the point and watershed-average scales. We evaluated the soil moisture estimates in terms of the root mean squared error (RMSE); unbiased root means squared error (ubRMSE); and Kling-Gupta efficiency (KGE; Kling et al., 2012). The KGE score combines the linear Pearson correlation (ρ), the bias component (β) defined by the ratio of estimated and observed means, and the variability component (γ) as the ratio of the estimated and observed coefficients of variation:

$$KGE = 1 - \sqrt{(\rho - 1)^2 + (\beta - 1)^2 + (\gamma - 1)^2} \quad (5)$$

$$\beta = \mu_{model}/\mu_{observation} \text{ and } \gamma = (\sigma_{model}/\mu_{model})/(\sigma_{observation}/\mu_{observation}) \quad (6)$$

where μ and σ are the distribution mean and standard deviation. To remove the impact of frozen soils in the evaluation, we masked the soil moisture estimates when the LSM soil temperature was below 0 °C.

In addition, to quantify the skill of the soil moisture products in representing the spatial variability of the observations, we calculated the spatial standard deviation for each watershed. The spatial standard deviation was calculated at each time step only when at least 10 in-situ observations and all the soil moisture products were available simultaneously. The entry data for each soil moisture product was identified based on the collocated grid cell of each in-situ observation.

2.5.2. Sensitivity analysis

As mentioned previously, the forecast bias between the satellite observed and modeled brightness temperature may lead to sub-optimal merging and therefore it should be removed a priori. We observed that, for different watersheds, the merged soil moisture estimates showed different performance with or without the long-term brightness temperature forecast bias removal. For instance, at some watersheds the

merging performed well without the forecast bias term, while for other watersheds, the merging performed very poorly without the forecast bias term. To investigate this disparity, we quantified the sensitivity of the downscaled soil moisture to the correction of the brightness temperature forecast bias by expanding Eq. (4) to include weights w_1 and w_2 :

$$x_t^+ = x_t^- + K [(y_t - Hx_t^-)w_1 - (bias_{forecast})w_2] \quad (7)$$

In specific, by varying the w_1 and w_2 weights, we quantified the sensitivity of the merged brightness temperature (x_t^+) with respect to the instantaneous contributions (via innovation term, $y_t - Hx_t^-$) and the long-term contributions via the forecast bias. In this way, the higher the w_1 weight, more weight is given to the instantaneous contributions of SMAP L3 brightness temperature. On the other hand, the higher the w_2 weight, more weight is given to the long-term contributions of the forecast bias (of HydroBlocks with respect to SMAP L3). This allows us to essentially investigate which temporal scale information that is contained in the observations we are allowing to influence the data merging. For this analysis we used the KGE, as well as the temporal soil moisture bias, variability, and correlation components to quantify the uncertainty in the retrieved downscaled soil moisture for each of the four watersheds. This analysis allows quantifying the errors associated with merging uncertain and biased model estimates and observations by accounting for the different contributions of the instantaneous and long-term temporal differences. Based on the outcomes of this sensitivity analysis, the results in this paper were carried out using a 0.5 weight for w_1 and w_2 .

3. Results

3.1. Merging and downscaling performance

Fig. 4 shows the time series of HydroBlocks LSM, SMAP L3, SMAP L4, and the downscaled soil moisture products averaged at the in-situ observation network locations and the respective collocated grid-cell for each watershed during 2016. HydroBlocks represented well the timing of the soil moisture peaks and the overall seasonal wet and dry dynamics with performance comparable or better to SMAP L3 and SMAP L4. However, SMAP L4, HydroBlocks, and the downscaled product generally overestimated soil moisture at dry sites, such as Walnut Gulch. SMAP L3 represented well the soil moisture dry downs in Little Washita and Walnut Gulch. SMAP L3 shows very high and low biases for the Little River and Reynolds Creek basins, respectively. Overall, in terms of temporal dynamics, the downscaled product offered a good compromise between HydroBlocks and SMAP L3 and L4 soil moisture products.

Fig. 5 shows the spatial distribution of soil moisture in terms of the annual mean for the HydroBlocks LSM, SMAP L3 and L4, the downscaled product, and the in-situ observations. As expected, the spatial heterogeneity accounted for by HydroBlocks is reflected in the spatial distribution of the downscaled soil moisture product. The model represented well the wet soil conditions at the valleys and river channels; as well as the drier agricultural fields surrounding the rivers in the Little Washita and Little River watersheds, and the high soil moisture spatial dynamics at the Little River watershed. The SMAP L3 retrievals, however, had only one or two grid cells covering each of the sites, with no spatial heterogeneity. SMAP L4 captures well the spatial pattern of drier and wetter conditions at Little Washita. The downscaled soil moisture follows the spatial pattern of HydroBlocks; however, the intensities are adjusted according to the merged SMAP L3 brightness temperature. Reynolds Creek showed to be the watershed where merging the SMAP L3 brightness temperature contributed the most. **Fig. 6** shows a zoom box of 10 km by 10 km of the merged soil moisture in each of the watersheds.

It is worth highlighting that **Fig. 5** shows the local impact on soil moisture of the merging of HydroBlocks and SMAP L3 brightness temperatures. However, the Gaussian operator (H), used in the

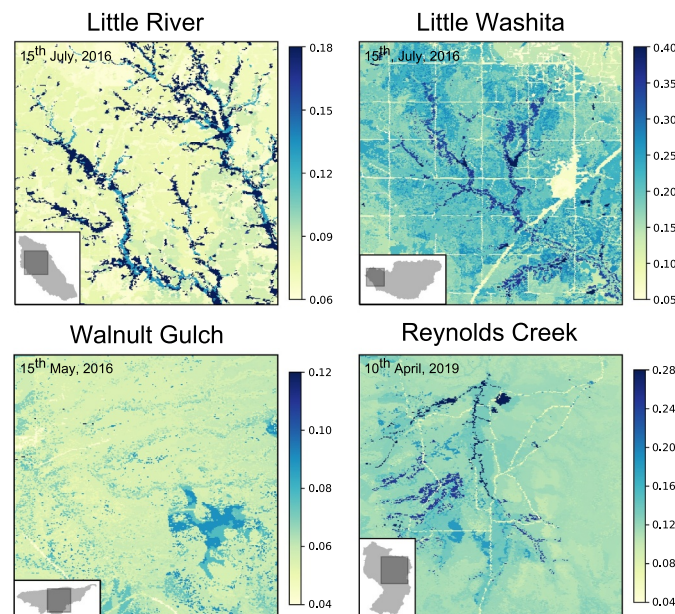


Fig. 6. The merged and downscaled soil moisture at Little River, Little Washita, Walnut Gulch, Reynolds Creek. Each panel shows the soil moisture zoomed in to a 10 km by 10 km domain area for a given time step.

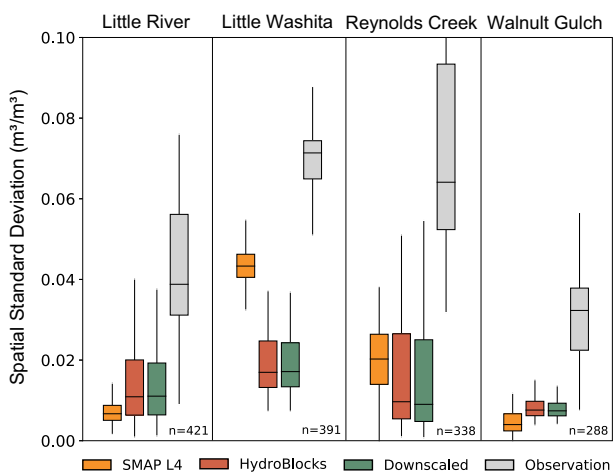


Fig. 7. Distribution of the soil moisture spatial standard deviation. The boxplots show the distribution of the soil moisture spatial standard deviation at each time step for the in-situ observations (grey) and the respective collocated grid cells of SMAP L4 (orange), HydroBlocks LSM (red), and the downscaled (green) soil moisture products. The spatial standard deviation at a given time was only calculated when data for at least 10 probes and the respective collocated grid cells were available simultaneously. The total number of data pairs in time for each watershed is reported in the bottom right of the graph.

merging, was applied to the brightness temperature within a 36-km radius from each HRU. In addition, SMAP and HydroBlocks used different clay content and surface temperature ancillary data. Because of the highly non-linear behavior of the soil dielectric properties, the relationship between the soil moisture before and after the merging is not always linear.

This spatial heterogeneity, shown in **Fig. 5** and **Fig. 6**, was quantified in terms of the spatial standard deviation. **Fig. 7** shows the distribution of the spatial standard deviation calculated at each time step for the in-situ probe and the collocated grid cell of each soil moisture product. We only calculated the spatial standard deviation at a given time when at least data of 10 probes and at the respective collocated grid cells were available simultaneously. SMAP L3 was not included in the analysis because each watershed only covers 1–2 grids. In comparison to SMAP L4, HydroBlocks often showed a higher spatial standard deviation. This spatial variability from HydroBlocks was also transferred to the downscaled product. The observed soil moisture spatial variability at all the watersheds was still much higher than that estimated by any of the soil moisture products, highlighting the lack of additional spatial dynamics that are still not being accounted.

In **Fig. 8**, we summarized the overall performance of the soil moisture products. The SMAP L3 performance varied significantly across the watersheds. At Walnut Gulch and Little Washita, SMAP L3 showed low bias, good correlation, and good KGE scores. But it performed poorly at Little River with a strong wet bias. SMAP L4 showed an overall low ubRMSE, but an overall high RMSE and coefficient of variations far from optimal, resulting in often the lowest KGE scores. HydroBlocks, on the other hand, performed well at cold to temperate and humid condition sites such as Reynolds Creek and Little River; but with poor performance at Little River and Walnut Gulch. These poor KGE performances are mostly driven by the bias ratio component, which is very sensitive to low soil moisture content. Nonetheless, the temporal dynamics and spatial distribution of the modeled and merged soil moisture at Walnut Gulch showed reasonable dynamics (**Fig. 4** and **Fig. 5**). The HydroBlocks model showed overall good skill in terms of temporal correlation and coefficient of variation. However, the model consistently overestimates soil moisture at all the sites except Little Washita.

The downscaled product presented a consistent lower RMSE and ubRMSE, averaging out the errors in both SMAP and HydroBlocks and

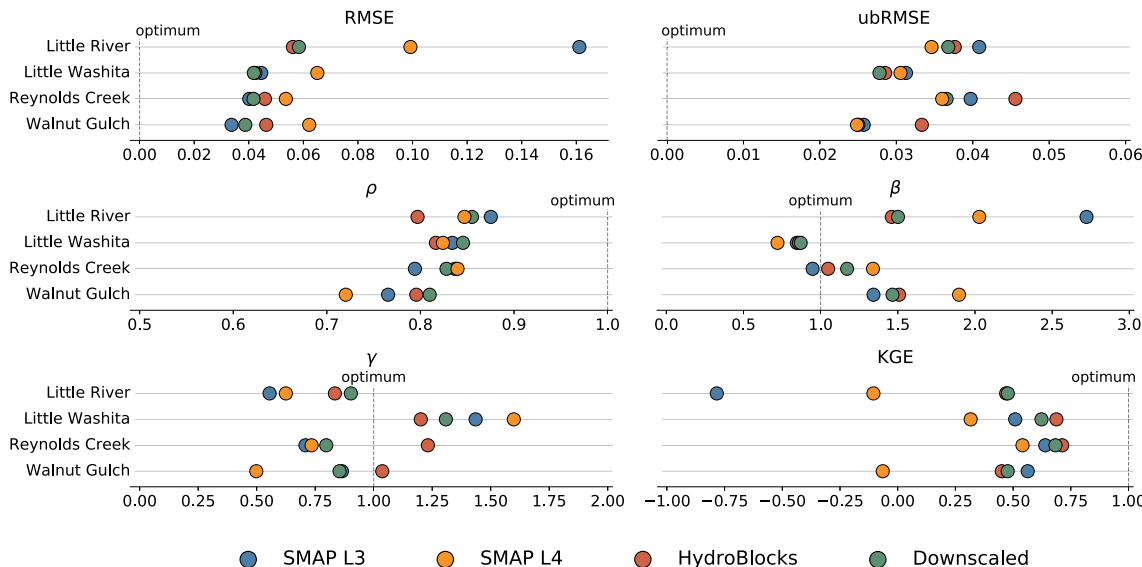


Fig. 8. Soil moisture evaluation against in-situ observations. We calculated the watershed spatial average using the soil moisture values at the collocated grid cell of the in-situ observations. The analysis covers the period between 2015 and 2017. The soil moisture products were evaluated in terms of its long-term mean squared error (RMSE) and the unbiased RMSE (ubRMSE); as well as the bias ratio (β), the variability ratio (γ), and the linear Pearson correlation (ρ), which represents the components of the Kling-Gupta score (KGE).

even improving both products' performance. Merging brightness temperatures observations improved soil moisture temporal correlation and ubRMSE in all the watersheds. However, the downscaled soil moisture often added value to the SMAP L3 estimates if the HydroBlocks performance is similar or higher than SMAP L3 estimates; otherwise, the performance is degraded, such as seen for Walnut Gulch. This was investigated further in the uncertainty analysis in Section 3.2. Although the downscaled product did not always perform the best in each metric individually, we observed an overall improvement of SMAP L3 and SMAP L4 estimates. The presented merging framework shows the potential to consolidate both SMAP and HydroBlocks estimates with an overall better accuracy than either independently. With respect to SMAP L3, the merged soil moisture showed the most substantial improvement in the Little River watershed, where the KGE score of SMAP rose from -0.78 to 0.47 .

The soil moisture performance at the in-situ level was evaluated in terms of the KGE score as a summary metric (Fig. 9). SMAP L3 performance was fairly consistent across all probes in each basin, either estimating the values very well as in Walnut Gulch or very poorly, as in Little River, with minimal spatial variability due to its coarse resolution. SMAP L4 showed to improve SMAP-L3 the performance is most of the sites, exception for Walnut Gulch. The merged product showed significant performance improvement in comparison to SMAP-L3 and SMAP-L4 at most of the in-situ sites. In comparison to HydroBlocks LSM, the merged product also shows overall improvement, but with smaller intensities. The exception is the Reynolds Creek, where SMAP-L3 merging degraded the model performance in some locations, but it still performed overall better than SMAP-L3 and SMAP-L4.

3.2. Sensitivity analysis of the merging framework

As seen in Fig. 8 and Fig. 9, the performance of the model and satellite soil moisture estimates varied from watershed to watershed. When the bias in the model or the satellite soil moisture estimates was significant, and we have no prior knowledge of which performs better at a given location, it is difficult to predict if the merged soil moisture will be better. As mentioned previously, this is a consequence of the bias between the modeled and satellite brightness temperatures that leads to non-optimal merging. Here we aim to assess how much the bias between the satellite and the model brightness temperature at different

temporal scales affects the uncertainty in the merged soil moisture retrieval. To this end, we quantified the temporal correlation, bias ratio, coefficient of variation ratio, and KGE score of the merged soil moisture when the brightness temperatures were merged using different w_1 weights on the instantaneous contributions (via the innovation) and different w_2 weights on the long-term contributions (via the forecast bias), as expanded in Eq. (7). Fig. 10 shows the results of this sensitivity analysis on the uncertainties associated with the merging framework using different temporal scales weights.

From Fig. 10, we can observe that the soil moisture temporal correlation was insensitive to changes in the instantaneous (w_1) and long-term (w_2) contributions when merging brightness temperature. However, when there is a bias between the observed and modeled brightness temperatures, there was a clear linear relationship that yields an optimal 1.0 bias ratio and variability ratio for a set of w_1 and w_2 weight pairs. This linear pattern can be also observed in the KGE score. In terms of the instantaneous and the long-term contributions of the brightness temperatures differences, the merged soil moisture was particularly sensitive to the model and satellite estimates at the Little River and Walnut Gulch watershed. At Walnut Gulch, HydroBlocks showed a wet bias and the SMAP L3 estimates were more similar to the observations, and as a result, the merged soil moisture performance was optimal at $w_1 = 1.0$ and $w_2 = 0.0$. Therefore, forecast bias correction would worse the performance at this site. For Little River, however, SMAP L3 showed a very high soil moisture bias, and HydroBlocks performed better across all metrics, with estimates very similar to the observations. For this watershed, the optimal merging performance was found when the forecast bias was added to the estimates with $w_1 = 0.5$ and $w_2 = 0.8$. Here, we clearly see that the forecast biases between the estimates favor HydroBlocks, but the non-zero mean anomaly leads to uncertainties in the data merging. For Little Washita and Reynolds Creek, the brightness temperature and soil moisture biases between HydroBlocks and SMAP were small, and therefore, the merged soil moisture was less sensitive to different weights on the innovation and forecast bias terms. Although there is a linear pattern in how KGE varies for w_1 and w_2 weights in Little River and Walnut Gulch, the intercept at which the w_1 and w_2 pair leads to higher performance of the merged soil moisture estimates varies from watershed to watershed. Based on the four watersheds evaluated, there is no optimal temporal weight across all the sites. Thus, the results of this study were carried out using a 0.5 weight for w_1 and w_2 as a compromise

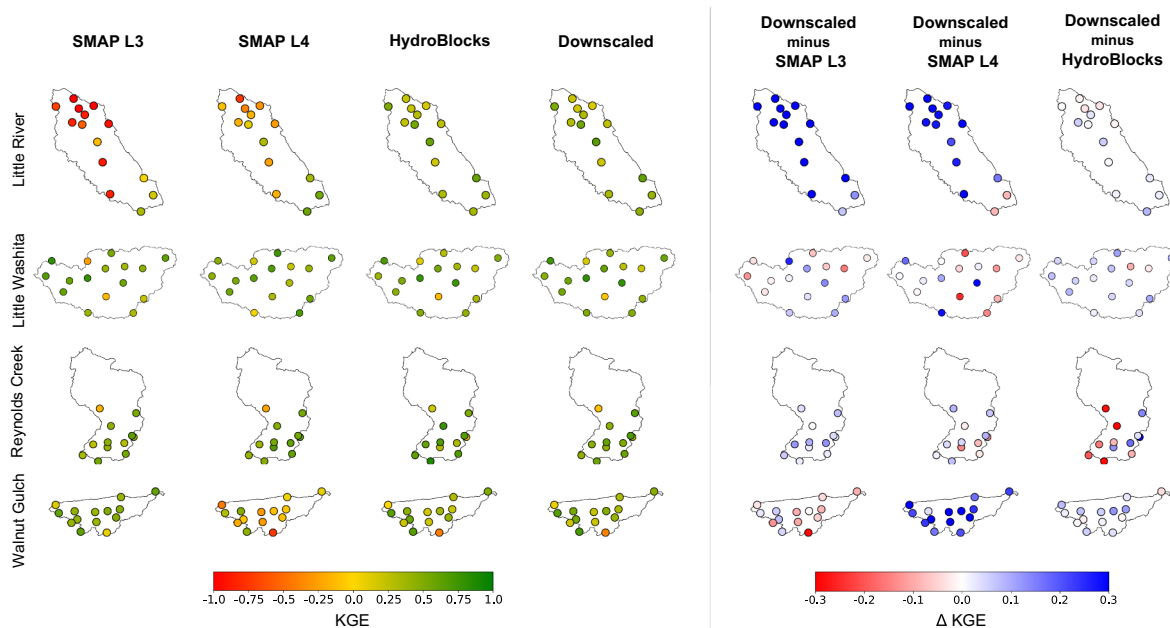


Fig. 9. KGE score of the soil moisture products evaluated against each in-situ probe. The columns show the KGE score for SMAP L3, the SMAP L4, HydroBlocks LSM, and the downscaled soil moisture. The best skill performance in terms of KGE is shown in green. The three last column shows the difference in KGE between the downscaled soil moisture and the SMAP L3, the SMAP L4, and the HydroBlocks LSM. The increase in performance is shown in blue.

between the instantaneous and the long-term contributions of the differences between the observed and the forecasted brightness temperatures. We discuss this in detail in Section 4.3.

4. Discussion

4.1. Overview of the strengths of the downscaling framework

We presented a merging framework to downscale soil moisture to an unprecedented 30-m spatial resolution. By using field-scale physically-based land surface modeling, the merged product takes into account the interaction of soil moisture with elevation, aspect, soil properties, vegetation, subsurface water dynamics, and climate. This is a critical benefit, because simulating land surface processes and these interactions at fine scales lead to an enhanced representation of the water and energy balances as well as carbon estimates (Piles et al., 2011; Falloon et al., 2011). These physical interactions are generally not accounted for when using machine learning and statistical downscaling approaches (Liu et al., 2017). In addition, our framework merges the directly observed brightness temperature instead of the post-processed soil moisture retrieval, which is subject to uncertainties and non-linearities within the RTM (discussed later in this subsection). The computational efficiency of the proposed framework is also a significant advantage. By clustering high-resolution proxies of the drivers of the landscape heterogeneity into HRUs, HydroBlocks efficiently accounts for most of the landscape spatial variability with a minimal computational cost, as demonstrated in Chaney et al. (2016).

In the context of using remote sensing to monitor hydrological processes, this work major contribution is a framework capable of modeling and merging hydrological estimates from field-scale to continental domains. Merging and potentially assimilating remotely sensed observations across different scales can contribute to elucidate the scaling behavior of hydrological processes from the point scale to the footprint scale of spaceborne sensors (Western et al., 2002). Proper characterization of the scaling behavior of hydrological processes, such as soil moisture, can aid the calibration and evaluation of RTMs and satellite retrieval products. Although here we introduce a merging and downscaling framework applied to each time step independently, this

work paves the way towards a hyper-resolution earth system modeling for multiscale dynamic data assimilation. The proposed HRU-based merging could be implemented with the system states and error covariances being updated sequentially, as it is done using traditional and ensemble Kalman filters, as well as other similar dynamic assimilation approaches (Lievens et al., 2016; Reichle et al., 2018a).

4.2. Uncertainties and caveats of the approach

Despite the promising results and potential further applications, the merging framework has limitations. In this section, we discuss the implications of the weaknesses of the land surface and radiative transfer model, as well as the uncertainties of the corresponding ancillary data.

4.2.1. Land surface modeling limitations

Modeled hydrological processes, including soil moisture, can be sensitive to uncertainties in the topography, land cover, soil properties, and meteorological input data, as well as to deficiencies of the physical process parameterizations in the LSM. Meteorological inputs, especially precipitation, are known to be one of the largest sources of uncertainties (Wanders et al., 2012; Beck et al., 2016). Although the 3-km NLDAS2-derived dataset accurately represented the temporal dynamics of the soil moisture peaks (Fig. 4), there is an overall wet bias in the model estimates (Fig. 7). Merging in-situ precipitation observations to the meteorological input data can reduce the soil moisture uncertainties, as demonstrated in Chaney et al. (2015). In addition, there are uncertainties related to the soil properties characterization and the process-representation of the soil-water hydraulics, as both control soil moisture levels and dry-down dynamics. The impact of these limitations is quantified in terms of the ubRMSE and the coefficient of variation in Fig. 7. The soil moisture estimates can also be impacted by misclassification of land cover as well as improper phenology and root structure representation (Dahlin et al., 2015), especially in dry conditions. In terms of model representativeness, a significant source of uncertainties is the lack of representation of human activities, such as irrigation, reservoir operation, groundwater pumping (Wanders and Wada, 2015; Pokhrel et al., 2017), that can dramatically influence soil moisture dynamics, especially at fine scales.

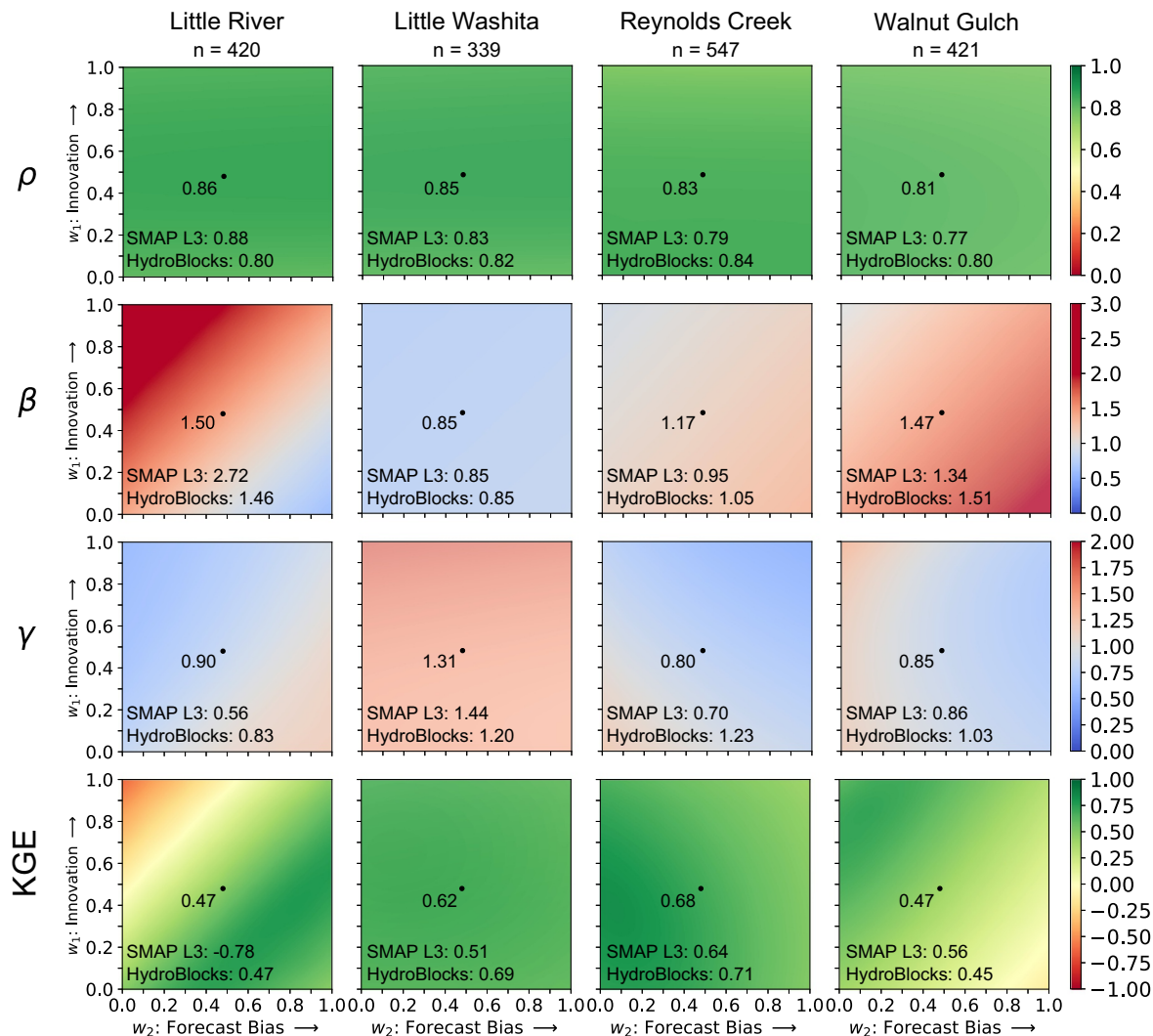


Fig. 10. The sensitivity of the merged soil moisture to changes in the contributions of the instantaneous and the long-term differences in model and observed brightness temperature. The sensitivity was performed by varying the weights in the innovation term (w_1) and the forecast bias term (w_2) when merging HydroBlocks-RTM and SMAP brightness temperatures. We evaluated the merged soil moisture using Pearson correlation, bias ratio, coefficient of variation ratio, and KGE score (lines) for each of the watersheds (columns). Each panel evaluates the merged soil moisture using different w_1 and w_2 values (varying from 0 to 1) in the brightness temperature merging. The central dot indicates the performance of the merged soil moisture product using 0.5 weight for w_1 and w_2 . For correlation and KGE, the optimal merging is shown in green; for the bias ratio and the variability component, the optimal is shown in grey.

While merging SMAP observations can help to better estimate soil moisture over largely irrigated domains, an alternative is to use more statistical data-driven approaches, such as proposed in Fang et al. (2019) and Ojha et al. (2019). More generally, a common way to overcome data and model limitations is to calibrate these soil-water parameters against soil moisture observations, river discharge, or even fine-scale, satellite-derived land surface temperature. Previously, Cai et al. (2017) showed that HydroBlocks soil moisture estimates have excellent performance under calibrated conditions. Here, however, we choose to follow an independent evaluation to assess the merged product skill at locations where there are high uncertainties in the ancillary data, or there is a lack of in-situ observations of soil moisture. A potential alternative to reduce the LSM uncertainties is the use of ensemble model simulations and ensemble Kalman filtering to account for the distribution of possible soil moisture states. However, this requires multiple LSM-RTM simulations and hence, will be computationally costly.

4.2.2. Radiative transfer modeling limitations

In terms of the radiative transfer modeling, uncertainties are mainly

due to the brightness temperature observations and ancillary remote sensing data used to parameterize the Tau-Omega brightness temperature RTM. The uncertainties in the measurements are linked to, among others, the inclination angle, the sensor penetration depth, the differences between the brightness temperature measured using the vertical and horizontal polarization, as well as the nature of the sensor retrieval that needs to be further gridded to a regular grid (O'Neill et al., 2018). Similar to LSMs, soil properties can influence the brightness temperature and soil moisture retrievals, as microwave measurements can penetrate deeper at increasing soil sand content and the presence of large macropores (Owe and Van de Griend, 1998; Casa et al., 2013). Soil emissivity properties also depend on accurately specified clay content for proper soil moisture estimates (Mironov et al., 2009). Vegetation and land cover characteristics also play a role, including uncertainties derived from land cover class, vegetation index, albedo, vegetation optical depth, and surface roughness. These ancillary data are often retrieved at a high resolution but aggregated to a coarser scale to match the footprint of the brightness temperature sensor. This is can be an issue for hyper-resolution RTM-based retrieval algorithms, as coarse-scale aggregated ancillary data (i) underestimates the spatial

heterogeneity of the landscape, and (ii) it may induce processes inconsistencies when data is combined with fine-scale LSM estimates, such as the soil moisture and surface temperature. We expect that higher resolution and better accuracy of albedo, vegetation optical depth, and roughness length would potentially lead to improvements in downscaled soil moisture performance. In addition, there are limitations with the Tau-Omega RTM itself. Schwank et al. (2018) discuss the current implementation of SMAP and SMOS Tau-Omega RTMs and its limitations over dense vegetation sites, among others. Due to these limitations, brightness temperature estimates from RTMs can be biased, requiring calibration to properly represent the soil moisture temporal dynamics (De Lannoy et al., 2013). In the context of hyper-resolution RTM modeling, further work is required to quantify the sensitivity and uncertainties of each of these coarse-scale RTM ancillary data within the HydroBlocks-RTM framework. Ideally, coupling HydroBlocks to an RTM that has been calibrated for fine-scale RTM ancillary data would improve the consistency between the modeled hydrological variables and the ancillary data, this may lead to improvements in the brightness temperature estimates, as well as improved performance of the final downscaled soil moisture.

4.3. General results and implications for soil moisture applications/transferringability

The proposed merging and downscaling framework represent the spatiotemporal dynamics of the soil moisture observations. As shown in Fig. 4 and Fig. 9, at the point and watershed levels, the merging framework consistently improves the SMAP L3 estimates. In addition, the downscaled product is able to represent the soil moisture spatial variability; with most of the contribution coming from HydroBlocks' spatial representation of the landscape heterogeneity (Fig. 5 and Fig. 7). An exception to the overall good performance is for the Walnut Gulch watershed, where neither the model, the merged soil moisture, and SMAP L4 was able to resolve the relatively high soil moisture bias ratio with the same performance of SMAP L3. SMAP L3 estimates are, however, known for their overall dry bias (Chan et al., 2018), and therefore tend to perform better in arid conditions. The lack of model skill in simulating hydrological processes in dry conditions is a general limitation of LSMs (Beck et al., 2016, 2017; Poltoradnev et al., 2018) but it can also be linked to biases in the meteorological estimates and the soil-water hydraulics limitations mentioned above. Further work is needed to understand if these results can be generalized across a broader set of dry environments.

The results showed that the merged soil moisture can be sensitive to changes in the contribution of the instantaneous and the long-term differences between the model and observed brightness temperatures (Fig. 10). This is the case for the Little River and Walnut Gulch watersheds where there was significant soil moisture and brightness temperature bias between the estimates, albeit that HydroBlocks performed very well on Little River, and SMAP performed very well on Walnut Gulch. In this context, at Walnut Gulch the instantaneous contributions (via the innovation term) provide more benefit to the merging than the long-term contributions (via the forecast bias term). Conversely, at Little River the merging benefited more from the long-term contributions than the instantaneous contribution. While the model and satellite performance vary from place to place, we adopted a 0.5 w_1 and w_2 weight as a compromise between the temporal contribution of the instantaneous and the long-term differences between observed and modeled brightness temperature. This pair of weights resulted in an overall improvement in SMAP performance, as shown in the evaluation results in Fig. 9 and Fig. 10.

The impact of the forecast bias between the model and satellite observation on the merged soil moisture has also been identified by previous SMAP and SMOS studies (Reichle et al., 2004; De Lannoy et al., 2007; Kumar et al., 2012). Similarly, a typical approach is to rescale the soil moisture time series by subtracting the standardized

forecast bias from the estimates before the assimilation (Reichle et al., 2004). For this study we used a 0.5 weight, however, a more consistent and transferable way forward is to consider which aspects of the landscape, hydroclimate, and human activities (i.e. irrigation) lead to the instantaneous and long-term differences between the model and satellite observations. If the contribution of the instantaneous and long-term brightness temperature differences can be modeled based on these aspects, this can potentially reduce the sensitivity of the merged soil moisture to uncertainties in the model and satellite estimates (Kolassa et al., 2017). In addition, extending the evaluation over a broader domain of soils, land cover, and climate conditions could provide further guidance on the skill and uncertainties of the soil moisture products, as shown in Draper et al. (2012).

5. Summary and conclusions

Soil moisture monitoring and prediction have essential implications for water management, but it is also one of the most challenging surface processes to predict. It varies highly in space and time, as a result of being tied to the spatial heterogeneity of the landscape in terms of topography, soil properties, land cover, and variations in microclimates. Several statistically and physically-based techniques to downscale soil moisture have been proposed (e.g., Peng et al., 2017), including using fully distributed land surface models (e.g. Sahoo et al., 2013; Garnaud et al., 2016). However, previously proposed downscaling techniques often do not physically represent the land surface processes in an integrated manner (i.e., statistical and machine learning based models) or do not account for the fine-scale heterogeneity of the landscape (i.e., coarse-scale global LSMs). In addition, model-based downscaling techniques relying on fully distributed hydrological models can be extremely computational costly when applied at fine-scales over continental domains.

In this work, we introduced a physically-based downscaling framework that combines hyper-resolution land surface modeling, radiative transfer modeling, and spatial Bayesian merging. Specifically, we take advantage of the HRU concept of hyper-resolution modeling to reduce the dimensionality of the system. This leads to efficient modeling and merging of remotely sensed hydrological processes. The proposed hyper-resolution assimilation concept can be extended to more robust multi-scale dynamic assimilation using, for instance, Ensemble Kalman filter. It can also be extended to assimilate other remotely sensed retrievals, with or without the need for coupling the LSM with an RTM. For instance, this HRU-based merging framework can be applied to assimilate the radiative observations via an RTM, as for retrievals of soil moisture, land surface temperature, and snow water equivalent. Or it can be applied to directly assimilate the remotely sensed retrievals without coupling the LSM to an RTM, as for estimates of evapotranspiration, canopy temperature, vegetation indices (i.e. LAI), groundwater storage, among others.

Here, we demonstrated this framework by downscaling SMAP soil moisture estimates to an unprecedented 30-m spatial resolution by coupling HydroBlocks LSM to a Tau-Omega RTM. The downscaled framework showed excellent performance in accounting for the soil moisture temporal dynamics and spatial heterogeneity. When compared to in-situ observations, the downscaled product showed a consistent overall high correlation above 0.81 and average KGE scores of 0.56, with better performance than SMAP-L3 and SMAP-L4 overall. We also quantified the sensitivity of the merging framework to the relative contribution of the instantaneous and the long-term differences in model and observed brightness temperature. The sensitivity analysis was performed by varying the weights in the innovation and forecast bias terms when merging HydroBlocks and SMAP brightness temperature. We found that a balance between the temporal contribution of the instantaneous and the long-term differences in brightness temperature yields an overall good soil moisture KGE score with added value to the SMAP estimates.

The proposed merging framework leverages SMAP potential by providing high-resolution and accurate soil moisture estimates that are relevant for field-scale water resources decision making. For instance, 30-m soil moisture data can improve estimates of agricultural yields and water demand at field scale (Ines et al., 2013; Fisher et al., 2017; Zhao et al., 2018; Waldman et al., 2019). If we fully trust SMAP estimates and do not bias correct the brightness temperature estimates, the 30- downscaled soil moisture can help track the large-scale impact of human activities, such as irrigation (Mathias et al., 2017; Lawston et al., 2017; Dirmeyer and Norton, 2018). The spatiotemporal distribution of soil moisture can help monitoring the spatial distribution of species (Tromp-van Meerveld and McDonnell, 2006; Reich et al., 2018), and epidemic diseases (Beck et al., 2000; Rinaldo et al., 2012). By taking into account the fine-scale variability of soil moisture extremes, fine-scale soil moisture can improve the forecast skill of extreme hydrologic events such as droughts (van Dijk et al., 2013; Sheffield et al., 2014; Sadri et al., 2018; Blyverket et al., 2019); wildfires (Taufik et al., 2017); as well as flooding and landslides by providing high-resolution estimates of antecedent soil moisture conditions (Ray and Jacobs, 2007; Pelletier et al., 1997). Fine-scale remotely sensed soil moisture estimates can also help better quantify the coupling between the surface and the atmosphere (Guillod et al., 2015; Taylor et al., 2012); as well as improve the soil moisture initialization conditions for numerical weather forecast systems (Dirmeyer and Halder, 2016).

The physically-based downscaling framework presented in this study allows for bridging the gap between coarse-scale satellite retrievals and fine-scale model simulations as we move towards “everywhere and locally relevant” prediction of hydroclimate processes. In future work, there is potential to expand this analysis over continental domains and assess the skill of the downscaling framework over a broader range of soil properties, topography, land cover, and hydroclimate conditions, as well as its applicability in helping solve key water resources challenges linked to soil moisture estimates.

Funding

This work was supported by NASA Soil Moisture Cal/Val Activities as a SMAP Mission Science Team Member (grant number NNX14AH92G); by the “Modernizing Observation Operator and Error Assessment for Assimilating In-situ and Remotely Sensed Snow/Soil Moisture Measurements into NWM” project from NOAA (grant number NA19OAR4590199); and the Princeton Environmental Institute at Princeton University through the Mary and Randall Hack ‘69 Research Fund Award.

CRediT authorship contribution statement

Noemi Vergopolan:Conceptualization, Methodology, Software, Formal analysis, Writing - original draft.**Nathaniel W. Chaney:**Software, Writing - original draft, Methodology.**Hylke E. Beck:**Writing - original draft.**Ming Pan:**Resources, Methodology, Writing - original draft.**Justin Sheffield:**Writing - original draft.**Steven Chan:**Resources.**Eric F. Wood:**Supervision, Conceptualization.

Declaration of competing interest

The authors declare that they have no known competing financial interests or personal relationships that could have appeared to influence the work reported in this paper.

References

- Anderson, B.D.O., Moore, J.B., 2005. Optimal Filtering. Dover Publications, Mineola.
- Andreadis, K.M., Lettenmaier, D.P., 2006. Assimilating remotely sensed snow observations into a macroscale hydrology model. *Adv. Water Resour.* 29, 872–886. <https://doi.org/10.1016/j.advwatres.2005.08.004>.
- Atkinson, P.M., 2013. Downscaling in remote sensing. *Int. J. Appl. Earth Obs. Geoinf.* 22, 106–114. <https://doi.org/10.1016/j.jag.2012.04.012>.
- Beck, L., Lobitz, B.M., Wood, B.L., 2000. Remote sensing and human health: new sensors and new opportunities. *Emerg. Infect. Dis.* 6, 217–227. <https://doi.org/10.3201/eid0603.000301>.
- Beck, H.E., van Dijk, A.I.J.M., de Roo, A., Dutra, E., Fink, G., Orth, R., Schellekens, J., 2016. Global evaluation of runoff from ten state-of-the-art hydrological models. *Hydrolog. Earth Syst. Sci. Discuss.* 1–33. <https://doi.org/10.5194/hess-2016-124>.
- Beck, H.E., Vergopolan, N., Pan, M., Levizzani, V., van Dijk, A.I.J.M., Weedon, G.P., Brocca, L., Pappenberger, F., Huffman, G.J., Wood, E.F., 2017. Global-scale evaluation of 22 precipitation datasets using gauge observations and hydrological modeling. *Hydrolog. Earth Syst. Sci.* 21, 6201–6217. <https://doi.org/10.5194/hess-21-6201-2017>.
- Bierkens, M.F.P., Bell, V.A., Burek, P., Chaney, N., Condon, L.E., David, C.H., de Roo, A., Döll, P., Drost, N., Famiglietti, J.S., Flörke, M., Goochis, D.J., Houser, P., Hut, R., Keune, J., Kollet, S., Maxwell, R.M., Reager, J.T., Samaniego, L., Sudicky, E., Sutardjaja, E.H., van de Giesen, N., Winsemius, H., Wood, E.F., 2015. Hyper-resolution global hydrological modelling: what is next? *Hydrolog. Process.* 29, 310–320. <https://doi.org/10.1002/hyp.10391>.
- Bindlish, R., Jackson, T.J., Wood, E., Gao, H., Starks, P., Bosch, D., Lakshmi, V., 2003. Soil moisture estimates from TRMM microwave imager observations over the southern United States. *Remote Sens. Environ.* 85, 507–515. [https://doi.org/10.1016/s0034-4257\(03\)00052-x](https://doi.org/10.1016/s0034-4257(03)00052-x).
- Blyverket, J., Hamer, P.D., Schneider, P., Albergel, C., Lahoz, W.A., 2019. Monitoring soil moisture drought over northern high latitudes from space. *Remote Sens.* 11 (10), 1200.
- Cai, X., Pan, M., Chaney, N.W., Colliander, A., Misra, S., Cosh, M.H., Crow, W.T., Jackson, T.J., Wood, E.F., 2017. Validation of SMAP soil moisture for the SMAPVEX15 field campaign using a hyper-resolution model. *Water Resour. Res.* 53, 3013–3028. <https://doi.org/10.1002/2016wr019967>.
- Casa, R., Castaldi, F., Pascucci, S., Palombo, A., Pignatti, S., 2013. A comparison of sensor resolution and calibration strategies for soil texture estimation from hyperspectral remote sensing. *Geoderma* 197–198, 17–26. <https://doi.org/10.1016/j.geoderma.2012.12.016>.
- Chan, S.K., Bindlish, R., O'Neill, P.E., Njoku, E., Jackson, T., Colliander, A., Chen, F., et al., 2016. Assessment of the SMAP passive soil moisture product. *IEEE Trans. Geosci. Remote Sens.* 54 (8), 4994–5007.
- Chan, S.K., Bindlish, R., O'Neill, P.E., Jackson, T., Njoku, E., Dunbar, S., Chaubell, J., Piepmeyer, J., Yueh, S., Entekhabi, D., Colliander, A., Chen, F., Cosh, M.H., Caldwell, T., Walker, J., Berg, A., McNairn, H., Thibeault, M., Martínez-Fernández, J., Uldall, F., Seyfried, M., Bosch, D., Starks, P., Holifield Collins, C., Prueger, J., van der Velde, R., Asanuma, J., Palecki, M., Small, E.E., Zreda, M., Calvet, J., Crow, W.T., Kerr, Y., 2018. Development and assessment of the SMAP enhanced passive soil moisture product. *Remote Sens. Environ.* 204, 931–941. <https://doi.org/10.1016/j.rse.2017.08.025>.
- Chaney, N.W., Roundy, J.K., Herrera-Estrada, J.E., Wood, E.F., 2015. High-resolution modeling of the spatial heterogeneity of soil moisture: applications in network design. *Water Resour. Res.* 51, 619–638. <https://doi.org/10.1002/2013wr014964>.
- Chaney, N.W., Metcalfe, P., Wood, E.F., 2016. HydroBlocks: field-scale resolving land surface model for application over continental extents. *Hydrolog. Process.* 30, 3543–3559. <https://doi.org/10.1002/hyp.10891>.
- Chaney, N.W., Van Huijgevoort, M.H.J., Shevliakova, E., Malyshev, S., Milly, P.C.D., Gauthier, P.P.G., Sulman, B.N., 2018. Harnessing big data to rethink land heterogeneity in earth system models. *Hydrolog. Earth Syst. Sci.* 22, 3311–3330. <https://doi.org/10.5194/hess-22-3311-2018>.
- Chaney, N.W., Minasny, B., Herman, J.D., Nauman, T.W., Brungard, C.W., Morgan, C.L.S., McBratney, A.B., Wood, E.F., Yimam, Y., 2019. POLARIS soil properties: 30-m probabilistic maps of soil properties over the contiguous United States. *Water Resour. Res.* 55, 2916–2938. <https://doi.org/10.1029/2018wr022797>.
- Clark, M.P., Slater, A.G., Barrett, A.P., Hay, L.E., McCabe, G.J., Rajagopalan, B., Leavesley, G.H., 2006. Assimilation of snow covered area information into hydrologic and land-surface models. *Adv. Water Resour.* 29, 1209–1221. <https://doi.org/10.1016/j.advwatres.2005.10.001>.
- Colliander, A., Jackson, T.J., Bindlish, R., Chan, S., Das, N., Kim, S.B., Cosh, M.H., Dunbar, R.S., Dang, L., Pashaian, L., Asanuma, J., Aida, K., Berg, A., Rowlandson, T., Bosch, D., Caldwell, T., Caylor, K., Goodrich, D., al Jassar, H., Lopez-Baeza, E., Martínez-Fernández, J., González-Zamora, A., Livingston, S., McNairn, H., Pacheco, A., Moghaddam, M., Montzka, C., Notarnicola, C., Niedrist, G., Pellarin, T., Prueger, J., Pulliajainen, J., Rautiainen, K., Ramos, J., Seyfried, M., Starks, P., Su, Z., Zeng, Y., van der Velde, R., Thibeault, M., Dorigo, W., Vreugdenhil, M., Walker, J.P., Wu, X., Monerris, A., O'Neill, P.E., Entekhabi, D., Njoku, E.G., Yueh, S., 2017. Validation of SMAP surface soil moisture products with core validation sites. *Remote Sens. Environ.* 191, 215–231. <https://doi.org/10.1016/j.rse.2017.01.021>.
- Colliander, A., Cosh, M.H., Misra, S., Jackson, T.J., Crow, W.T., Powers, J., McNairn, H., Bullock, P., Berg, A., Magagi, R., Gao, Y., Bindlish, R., Williamson, R., Ramos, I., Latham, B., O'Neill, P., Yueh, S., 2019. Comparison of high-resolution airborne soil moisture retrievals to SMAP soil moisture during the SMAP validation experiment 2016 (SMAPVEX16). *Remote Sens. Environ.* 227, 137–150. <https://doi.org/10.1016/j.rse.2019.04.004>.
- Crow, W.T., Van Loon, E., 2006. Impact of incorrect model error assumptions on the sequential assimilation of remotely sensed surface soil moisture. *J. Hydrometeorol.* 7, 421–432. <https://doi.org/10.1175/jhm499.1>.
- Crow, W.T., Berg, A.A., Cosh, M.H., Loew, A., Mohanty, B.P., Panciera, R., de Rosnay, P., Ryu, D., Walker, J.P., 2012. Upscaling sparse ground-based soil moisture observations for the validation of coarse-resolution satellite soil moisture products. *Rev. Geophys.* 50. <https://doi.org/10.1029/2011rg000372>.

- Dahlin, K.M., Fisher, R.A., Lawrence, P.J., 2015. Environmental drivers of drought deciduous phenology in the community land model. *Biogeosci. Discuss.* 12, 5803–5839. <https://doi.org/10.5194/bgd-12-5803-2015>.
- De Lannoy, G.J.M., Reichle, R.H., 2016a. Assimilation of SMOS brightness temperatures or soil moisture retrievals into a land surface model. *Hydrol. Earth Syst. Sci. Discuss.* 1–27. <https://doi.org/10.5194/hess-2016-414>.
- De Lannoy, G.J., Reichle, R.H., 2016b. Global assimilation of multi-angle and multi-polarization SMOS brightness temperature observations into the GEOS-5 catchment land surface model for soil moisture estimation. *J. Hydrometeorol.* 17 (2), 669–691.
- De Lannoy, G.J., Reichle, R.H., Houser, P.R., Pauwels, V.R., Verhoest, N.E., 2007. Correcting for forecast bias in soil moisture assimilation with the ensemble Kalman filter. *Water Resour. Res.* 43 (9).
- De Lannoy, G.J.M., Reichle, R.H., Arsenault, K.R., Houser, P.R., Kumar, S., Verhoest, N.E.C., Pauwels, V.R.N., 2012. Multiscale assimilation of advanced microwave scanning radiometer-EOS snow water equivalent and moderate resolution imaging spectroradiometer snow cover fraction observations in northern Colorado. *Water Resour. Res.* 48. <https://doi.org/10.1029/2011wr010588>.
- De Lannoy, G.J., Reichle, R.H., Pauwels, V.R., 2013. Global calibration of the GEOS-5 L-band microwave radiative transfer model over non-frozen land using SMOS observations. *J. Hydrometeorol.* 14 (3), 765–785.
- van Dijk, A.I.J.M., Beck, H.E., Crosbie, R.S., de Jeu, R.A.M., Liu, Y.Y., Podger, G.M., Timbal, B., Viney, N.R., 2013. The millennium drought in southeast Australia (2001–2009): natural and human causes and implications for water resources, ecosystems, economy, and society. *Water Resour. Res.* 49, 1040–1057. <https://doi.org/10.1002/wrcr.20123>.
- Dirmeyer, P.A., Halder, S., 2016. Sensitivity of numerical weather forecasts to initial soil moisture variations in CFSv2. *Weather Forecast.* 31 (6), 1973–1983.
- Dirmeyer, P., Norton, H., 2018. Indications of surface and sub-surface hydrologic properties from SMAP soil moisture retrievals. *Hydrology* 5, 36. <https://doi.org/10.3390/hydrology5030036>.
- Draper, C.S., Reichle, R.H., De Lannoy, G.J.M., Liu, Q., 2012. Assimilation of passive and active microwave soil moisture retrievals. *Geophys. Res. Lett.* 39, L04401. <https://doi.org/10.1029/2011GL050655>.
- Drusch, M., Wood, E.F., Gao, H., 2005. Observation operators for the direct assimilation of TRMM microwave imager retrieved soil moisture. *Geophys. Res. Lett.* 32. <https://doi.org/10.1029/2005gl023623>.
- Durand, M., Margulis, S.A., 2006. Feasibility test of multifrequency radiometric data assimilation to estimate snow water equivalent. *J. Hydrometeorol.* 7, 443–457. <https://doi.org/10.1175/jhm502.1>.
- Entekhabi, D., Yuch, S., O'Neill, P.E., Kellogg, K.H., Allen, A., Bindlish, R., Brown, M., Chan, S., Colliander, A., Crow, W.T., Das, N., 2014. SMAP Handbook—Soil Moisture Active Passive: Mapping Soil Moisture and Freeze/Thaw from Space.
- Falloon, P., Jones, C.D., Ades, M., Paul, K., 2011. Direct soil moisture controls of future global soil carbon changes: an important source of uncertainty. *Glob. Biogeochem. Cycles* 25. <https://doi.org/10.1029/2010gb003938>. n/a-n/a.
- Fang, B., Lakshmi, V., Jackson, T.J., Bindlish, R., Colliander, A., 2019. Passive/active microwave soil moisture change disaggregation using SMAPVEX12 data. *J. Hydrol.* 574, 1085–1098.
- Farr, T.G., Rosen, P.A., Caro, E., Crippen, R., Duren, R., Hensley, S., Kobrick, M., Paller, M., Rodriguez, E., Roth, L., Seal, D., Shaffer, S., Shimada, J., Umland, J., Werner, M., Oskin, M., Burbank, D., Alsdorf, D., 2007. The shuttle radar topography mission. *Rev. Geophys.* 45. <https://doi.org/10.1029/2005rg000183>.
- Fisher, J.B., Melton, F., Middleton, E., Hain, C., Anderson, M., Allen, R., McCabe, M.F., Hook, S., Baldocchi, D., Townsend, P.A., Kilic, A., Tu, K., Miralles, D.D., Perret, J., Lagouarde, J.-P., Waliser, D., Purdy, A.J., French, A., Schimel, D., Famiglietti, J.S., Stephens, G., Wood, E.F., 2017. The future of evapotranspiration: global requirements for ecosystem functioning, carbon and climate feedbacks, agricultural management, and water resources. *Water Resour. Res.* 53, 2618–2626. <https://doi.org/10.1002/2016wr020175>.
- Garnaud, C., Bélair, S., Berg, A., Rowlandson, T., 2016. Hyperresolution land surface modeling in the context of SMAP Cal-Val. *J. Hydrometeorol.* 17, 345–352. <https://doi.org/10.1175/jhm-d-15-0070.1>.
- Ghent, D., Kaduk, J., Remedios, J., Ardö, J., Balzter, H., 2010. Assimilation of land surface temperature into the land surface model JULES with an ensemble Kalman filter. *J. Geophys. Res.* 115. <https://doi.org/10.1029/2010jd014392>.
- Guillod, B.P., Orlowsky, B., Miralles, D.G., Teuling, A.J., Seneviratne, S.I., 2015. Reconciling spatial and temporal soil moisture effects on afternoon rainfall. *Nat. Commun.* 6. <https://doi.org/10.1038/ncomms7443>.
- Hansen, M.C., Potapov, P.V., Moore, R., Hancher, M., Turubanova, S.A., Tyukavina, A., Thau, D., Stehman, S.V., Goetz, S.J., Loveland, T.R., Kommareddy, A., Egorov, A., Chini, L., Justice, C.O., Townshend, J.R.G., 2013. High-resolution global maps of 21st-century forest cover change. *Science* 342 (6160), 850–853. <https://doi.org/10.1126/science.1244693>.
- Homer, C.G., Dewitz, J., Yang, L., Jin, S., Danielson, P., Xian, G.Z., Coulston, J., Herold, N., Wickham, J., Megown, K., 2015. Completion of the 2011 National Land Cover Database for the conterminous United States – representing a decade of land cover change information. *Photogramm. Eng. Remote. Sens.* 81, 345–354.
- Huang, C., Li, X., Lu, L., 2008. Retrieving soil temperature profile by assimilating MODIS LST products with ensemble Kalman filter. *Remote Sens. Environ.* 112, 1320–1336. <https://doi.org/10.1016/j.rse.2007.03.028>.
- Ines, A.V.M., Das, N.N., Hansen, J.W., Njoku, E.G., 2013. Assimilation of remotely sensed soil moisture and vegetation with a crop simulation model for maize yield prediction. *Remote Sens. Environ.* 138, 149–164. <https://doi.org/10.1016/j.rse.2013.07.018>.
- Jackson, T.J., 1993. III. Measuring surface soil moisture using passive microwave remote sensing. *Hydrol. Process.* 7, 139–152. <https://doi.org/10.1002/hyp.3360070205>.
- de Jeu, R.A.M., Wagner, W., Holmes, T.R.H., Dolman, A.J., van de Giesen, N.C., Friesen, J., 2008. Global soil moisture patterns observed by space borne microwave radiometers and scatterometers. *Surv. Geophys.* 29, 399–420. <https://doi.org/10.1007/s10712-008-9044-0>.
- Jones, M.O., Jones, L.A., Kimball, J.S., McDonald, K.C., 2011. Satellite passive microwave remote sensing for monitoring global land surface phenology. *Remote Sens. Environ.* 115, 1102–1114. <https://doi.org/10.1016/j.rse.2010.12.015>.
- Karthikeyan, L., Pan, M., Wanders, N., Kumar, D.N., Wood, E.F., 2017. Four decades of microwave satellite soil moisture observations: part 1. A review of retrieval algorithms. *Adv. Water Resour.* 109, 106–120. <https://doi.org/10.1016/j.advwatres.2017.09.006>.
- Kling, H., Fuchs, M., Paulin, M., 2012. Runoff conditions in the upper Danube basin under an ensemble of climate change scenarios. *J. Hydrol.* 424, 264–277.
- Kolassa, J., Reichle, R., Liu, Q., Cosh, M., Bosch, D., Caldwell, T., Colliander, A., Holifield Collins, C., Jackson, T., Livingston, S., Moghaddam, M., 2017. Data assimilation to extract soil moisture information from SMAP observations. *Remote Sens.* 9 (11), 1179.
- Koster, R.D., Suarez, M.J., 1992. Modeling the land surface boundary in climate models as a composite of independent vegetation stands. *J. Geophys. Res.* 97, 2697. <https://doi.org/10.1029/91jd01696>.
- Koster, R.D., Suarez, M.J., Ducharme, A., Stieglitz, M., Kumar, P., 2000. A catchment-based approach to modeling land surface processes in a general circulation model: 1. Model structure. *J. Geophys. Res.* 105, 24809–24822. <https://doi.org/10.1029/2000JD900327>.
- Kumar, S.V., Reichle, R.H., Harrison, K.W., Peters-Lidard, C.D., Yatheendradas, S., Santanello, J.A., 2012. A comparison of methods for a priori bias correction in soil moisture data assimilation. *Water Resour. Res.* 48 (3).
- Lawston, P.M., Santanello, J.A., Kumar, S.V., 2017. Irrigation signals detected from SMAP soil moisture retrievals. *Geophys. Res. Lett.* 44, 11,860–11,867. <https://doi.org/10.1002/2017gl075733>.
- Lievens, H., De Lannoy, G.J.M., Al Bitar, A., Drusch, M., Dumedah, G., Hendricks Franssen, H.-J., Kerr, Y.H., Tomer, S.K., Martens, B., Merlin, O., Pan, M., Roundy, J.K., Vereecken, H., Walker, J.P., Wood, E.F., Verhoest, N.E.C., Pauwels, V.R.N., 2016. Assimilation of SMOS soil moisture and brightness temperature products into a land surface model. *Remote Sens. Environ.* 180, 292–304. <https://doi.org/10.1016/j.rse.2015.10.033>.
- Lievens, H., Reichle, R.H., Liu, Q., De Lannoy, G.J.M., Dunbar, R.S., Kim, S.B., Das, N.N., Cosh, M., Walker, J.P., Wagner, W., 2017. Joint Sentinel-1 and SMAP data assimilation to improve soil moisture estimates. *Geophys. Res. Lett.* 44 (12), 6145–6153.
- Liu, Y., Yang, Y., Jing, W., Yue, X., 2017. Comparison of different machine learning approaches for monthly satellite-based soil moisture downscaling over Northeast China. *Remote Sens.* 10, 31. <https://doi.org/10.3390/rs10010031>.
- Mathias, S.A., Sorenson, J.P.R., Butler, A.P., 2017. Soil moisture data as a constraint for groundwater recharge estimation. *J. Hydrol.* 552, 258–266. <https://doi.org/10.1016/j.jhydrol.2017.06.040>.
- Mironov, V.L., Kosolapova, L.G., Fomin, S.V., 2009. Physically and mineralogically based spectroscopic dielectric model for moist soils. *IEEE Trans. Geosci. Remote Sens.* 47, 2059–2070. <https://doi.org/10.1109/tgrs.2008.2011631>.
- Niu, G.-Y., Yang, Z.-L., Mitchell, K.E., Chen, F., Ek, M.B., Barlage, M., Kumar, A., Manning, K., Niayogi, D., Rosero, E., Tewari, M., Xia, Y., 2011. The community Noah land surface model with multiparameterization options (Noah-MP): 1. Model description and evaluation with local-scale measurements. *J. Geophys. Res.* 116. <https://doi.org/10.1029/2010jd015139>.
- Njoku, E.G., Li, L., 1999. Retrieval of land surface parameters using passive microwave measurements at 6–18 GHz. *IEEE Trans. Geosci. Remote Sens.* 37, 79–93. <https://doi.org/10.1109/36.739125>.
- Norman, J.M., Anderson, M.C., Kustas, W.P., French, A.N., Mecikalski, J., Torn, R., Diak, G.R., Schmugge, T.J., Tanner, B.C.W., 2003. Remote sensing of surface energy fluxes at 101-m pixel resolutions. *Water Resour. Res.* 39. <https://doi.org/10.1029/2002wr001775>.
- O'Neill, P., Chan, S., Njoku, E., Jackson, T., Bindlish, R., 2014. Algorithm Theoretical Basis Document Level 2 & 3 Soil Moisture (Passive) Data Products, JPL D-66480, Jet Propul. Laboratories of the California Institute of Technology, Pasadena, CA, USA.
- Ojha, N., Merlin, O., Molero, B., Suere, C., Olivera-Guerra, L., Ait Hssaine, B., Amazirh, A., Al Bitar, A., Escorihuela, M.J., Er-Raki, S., 2019. Stepwise disaggregation of SMAP soil moisture at 100 m resolution using Landsat-7/8 data and a varying intermediate resolution. *Remote Sens.* 11 (16), 1863.
- O'Neill, P.E., Chan, S., Njoku, E., Jackson, T., Bindlish, R., 2018. SMAP L3 Radiometer Global Daily 36 km EASE-Grid Soil Moisture, Version 5. NASA National Snow and Ice Data Center Distributed Active Archive Center, Boulder, Colorado USA. <https://doi.org/10.5067/ZX7VXX2YLHED>.
- Owe, M., Van de Griend, A.A., 1998. Comparison of soil moisture penetration depths for several bare soils at two microwave frequencies and implications for remote sensing. *Water Resour. Res.* 34, 2319–2327. <https://doi.org/10.1029/98wr01469>.
- Pachepsky, David, Radcliffe, Elliott, Magdi Selim, H., 2003. Scaling Methods in Soil Physics. Crc Press, Boca Raton, Fla.
- Painter, T.H., Berisford, D.F., Boardman, J.W., Bormann, K.J., Deems, J.S., Gehrke, F., Hedrick, A., Joyce, M., Laidlaw, R., Marks, D., Mattmann, C., McGurk, B., Ramirez, P., Richardson, M., Skiles, S.M., Seidel, F.C., Winstral, A., 2016. The airborne snow observatory: fusion of scanning lidar, imaging spectrometer, and physically-based modeling for mapping snow water equivalent and snow albedo. *Remote Sens. Environ.* 184, 139–152. <https://doi.org/10.1016/j.rse.2016.06.018>.
- Pan, M., Wood, E.F., 2010. Impact of accuracy, spatial availability, and revisit time of satellite-derived surface soil moisture in a multiscale ensemble data assimilation system. *IEEE Journal of Selected Topics in Applied Earth Observations and Remote Sensing* 3, 49–56. <https://doi.org/10.1109/jstars.2010.2040585>.
- Pan, M., Sahoo, A.K., Wood, E.F., 2014. Improving soil moisture retrievals from a

- physically-based radiative transfer model. *Remote Sens. Environ.* 140, 130–140. <https://doi.org/10.1016/j.rse.2013.08.020>.
- Pan, M., Cai, X., Chaney, N.W., Entekhabi, D., Wood, E.F., 2016. An initial assessment of SMAP soil moisture retrievals using high-resolution model simulations and in situ observations. *Geophys. Res. Lett.* 43, 9662–9668. <https://doi.org/10.1002/2016gl069964>.
- Pelletier, J.D., Malamud, B.D., Blodgett, T., Turcotte, D.L., 1997. Scale-invariance of soil moisture variability and its implications for the frequency-size distribution of landslides. *Eng. Geol.* 48, 255–268. [https://doi.org/10.1016/s0013-7952\(97\)00041-0](https://doi.org/10.1016/s0013-7952(97)00041-0).
- Peng, J., Loew, A., Merlin, O., Verhoest, N.E.C., 2017. A review of spatial downscaling of satellite remotely sensed soil moisture. *Rev. Geophys.* 55, 341–366. <https://doi.org/10.1002/2016rg000543>.
- Piepmeier, J.R., Focardi, P., Horgan, K.A., Knuble, J., Ehsan, N., Lucey, J., Brambora, C., Brown, P.R., Hoffman, P.J., French, R.T., Mikhaylov, R.L., 2017. SMAP L-band microwave radiometer instrument design and first year on orbit. *IEEE Trans. Geosci. Remote Sens.* 55 (4), 1954–1966.
- Piles, M., Camps, A., Vall-llossera, M., Corbella, I., Panciera, R., Rudiger, C., Kerr, Y.H., Walker, J., 2011. Downscaling SMOS-derived soil moisture using MODIS visible/infrared data. *IEEE Trans. Geosci. Remote Sens.* 49, 3156–3166. <https://doi.org/10.1109/tgrs.2011.2120615>.
- Pokhrel, Y.N., Felfelani, F., Shin, S., Yamada, T.J., Satoh, Y., 2017. Modeling large-scale human alteration of land surface hydrology and climate. *Geoscience Letters* 4. <https://doi.org/10.1186/s40562-017-0076-5>.
- Poltoradnev, M., Ingwersen, J., Imukova, K., Högy, P., Wizemann, H.-D., Streck, T., 2018. How well does Noah-MP simulate the regional mean and spatial variability of topsoil water content in two agricultural landscapes in Southwest Germany? *J. Hydrometeorol.* 19, 555–573. <https://doi.org/10.1175/jhm-d-17-0169.1>.
- Ray, R.L., Jacobs, J.M., 2007. Relationships among remotely sensed soil moisture, precipitation and landslide events. *Nat. Hazards* 43, 211–222. <https://doi.org/10.1007/s10669-006-9095-9>.
- Reich, P.B., Sendall, K.M., Stefanski, A., Rich, R.L., Hobbie, S.E., Montgomery, R.A., 2018. Effects of climate warming on photosynthesis in boreal tree species depend on soil moisture. *Nature* 562, 263–267. <https://doi.org/10.1038/s41586-018-0582-4>.
- Reichle, R.H., 2008. Data assimilation methods in the earth sciences. *Adv. Water Resour.* 31, 1411–1418. <https://doi.org/10.1016/j.advwatres.2008.01.001>.
- Reichle, R.H., Koster, R.D., Dong, J., Berg, A.A., 2004. Global soil moisture from satellite observations, land surface models, and ground data: implications for data assimilation. *J. Hydrometeorol.* 5, 430–442. [https://doi.org/10.1175/1525-7541\(2004\)005<0430:gsmfo>2.0.co;2](https://doi.org/10.1175/1525-7541(2004)005<0430:gsmfo>2.0.co;2).
- Reichle, R.H., Kumar, S.V., Mahanama, S.P.P., Koster, R.D., Liu, Q., 2010. Assimilation of satellite-derived skin temperature observations into land surface models. *J. Hydrometeorol.* 11, 1103–1122. <https://doi.org/10.1175/2010jhm1262.1>.
- Reichle, R.H., De Lannoy, G.J.M., Forman, B.A., Draper, C.S., Liu, Q., 2014. Connecting satellite observations with water cycle variables through land data assimilation: examples using the NASA GEOS-5 LDAS. *Surv. Geophys.* 35, 577–606. <https://doi.org/10.1007/s10712-013-9220-8>.
- Reichle, R.H., De Lannoy, G.J., Liu, Q., Ardizzone, J.V., Colliander, A., Conaty, A., Crow, W., Jackson, T.J., Jones, L.A., Kimball, J.S., Koster, R.D., Mahanama, S.P., Smith, E.B., Berg, A., Bircher, S., Bosch, D., Caldwell, T.G., Cosh, M., González-Zamora, Á., Holifield Collins, C.D., Jensen, K.H., Livingston, S., Lopez-Baeza, E., Martínez-Fernández, J., McNairn, H., Moghaddam, M., Pacheco, A., Pellarin, T., Prueger, J., Rowlandson, T., Seyfried, M., Starks, P., Su, Z., Thibeault, M., van der Velde, R., Walker, J., Wu, X., Zeng, Y., 2017. Assessment of the SMAP level-4 surface and root-zone soil moisture product using in situ measurements. *J. Hydrometeorol.* 18, 2621–2645. <https://doi.org/10.1175/JHM-D-17-0063.1>.
- Reichle, R., De Lannoy, G., Koster, R.D., Crow, W.T., Kimball, J.S., Liu, Q., 2018a. SMAP L4 Global 3-hourly 9 km EASE-Grid Surface and Root Zone Soil Moisture Analysis Update, Version 4. NASA National Snow and Ice Data Center Distributed Active Archive Center, Boulder, Colorado USA. <https://doi.org/10.5067/60HB8VIP2T8W.11/01/2019>.
- Reichle, Rolf H., Liu, Qing, Koster, Randal D., Ardizzone, Joseph V., Colliander, Andreas, Crow, Wade T., Lannoy, Gabrielle J. De, Kimball, John S., 2018b. Soil Moisture Active Passive (SMAP) Project Assessment Report for Version 4 of the L4_SM Data Product.
- Rinaldo, A., Bertuzzo, E., Mari, L., Righetto, L., Blokesch, M., Gatto, M., Casagrandi, R., Murray, M., Vesenbeckh, S.M., Rodriguez-Iturbe, I., 2012. Reassessment of the 2010–2011 Haiti cholera outbreak and rainfall-driven multiseason projections. *Proc. Natl. Acad. Sci.* 109, 6602–6607. <https://doi.org/10.1073/pnas.120333109>.
- Roy, David P., et al., 2010. Web-enabled Landsat Data (WELD): Landsat ETM+ composite mosaics of the conterminous United States. *Remote Sens. Environ.* 114 (1), 35–49.
- Sadeghi, M., Babaeian, E., Tuller, M., Jones, S.B., 2017. The optical trapezoid model: a novel approach to remote sensing of soil moisture applied to Sentinel-2 and Landsat-8 observations. *Remote Sens. Environ.* 198, 52–68.
- Sadri, S., Wood, E.F., Pan, M., 2018. Developing a drought-monitoring index for the contiguous US using SMAP. *Hydroclim. Earth Syst. Sci.* 22, 6611–6626. <https://doi.org/10.5194/hess-22-6611-2018>.
- Sahoo, A.K., De Lannoy, G.J.M., Reichle, R.H., Houser, P.R., 2013. Assimilation and downscaling of satellite observed soil moisture over the Little River Experimental Watershed in Georgia, USA. *Adv. Water Resour.* 52, 19–33. <https://doi.org/10.1016/j.advwatres.2012.08.007>.
- Salmon, J.M., Friedl, M.A., Frolik, S., Wisser, D., Douglas, E.M., 2015. Global rain-fed, irrigated, and paddy croplands: A new high resolution map derived from remote sensing, crop inventories and climate data. *Int. J. Appl. Earth Obs. Geoinf.* 38, 321–334.
- Schwanck, M., Naderpour, R., Mätzler, C., 2018. “Tau-omega”- and two-stream emission models used for passive L-band retrievals: application to close-range measurements over a Forest. *Remote Sens.* 10, 1868. <https://doi.org/10.3390/rs10121868>.
- Sheffield, J., Wood, E.F., Chaney, N., Guan, K., Sadri, S., Yuan, X., Olang, L., Amani, A., Ali, A., Demuth, S., Ogollo, L., 2014. A drought monitoring and forecasting system for sub-Saharan African water resources and food security. *Bull. Am. Meteorol. Soc.* 95 (6), 861–882.
- Srivastava, P.K., Han, D., Ramirez, M.R., Islam, T., 2013. Machine learning techniques for downscaling SMOS satellite soil moisture using MODIS land surface temperature for hydrological application. *Water Resour. Manag.* 27, 3127–3144. <https://doi.org/10.1007/s11269-013-0337-9>.
- Taufik, M., Torfs, P.J.J.F., Uijlenhoet, R., Jones, P.D., Murdiyarto, D., Van Lanen, H.A.J., 2017. Amplification of wildfire area burnt by hydrological drought in the humid tropics. *Nat. Clim. Chang.* 7, 428–431. <https://doi.org/10.1038/nclimate3280>.
- Taylor, C.M., de Jeu, R.A.M., Guichard, F., Harris, P.P., Dorigo, W.A., 2012. Afternoon rain more likely over drier soils. *Nature* 489, 423–426. <https://doi.org/10.1038/nature11377>.
- Tromp-van Meerveld, H.J., McDonnell, J.J., 2006. On the interrelations between topography, soil depth, soil moisture, transpiration rates and species distribution at the hillslope scale. *Adv. Water Resour.* 29, 293–310. <https://doi.org/10.1016/j.advwatres.2005.02.016>.
- Waldman, K.B., Vergopolan, N., Attari, S.Z., Sheffield, J., Estes, L.D., Caylor, K.K., Evans, T.P., 2019. Cognitive biases about climate variability in smallholder farming systems in Zambia. *Weather, Climate, and Society* 11, 369–383. <https://doi.org/10.1175/wcas-d-18-0050.1>.
- Wanders, N., Wada, Y., 2015. Human and climate impacts on the 21st century hydrological drought. *J. Hydrol.* 526, 208–220. <https://doi.org/10.1016/j.jhydrol.2014.10.047>.
- Wanders, N., Karssenberg, D., Bierkens, M., Parinussa, R., de Jeu, R., van Dam, J., de Jong, S., 2012. Observation uncertainty of satellite soil moisture products determined with physically-based modeling. *Remote Sens. Environ.* 127, 341–356. <https://doi.org/10.1016/j.rse.2012.09.004>.
- Western, A.W., Grayson, R.B., Blöschl, G., 2002. Scaling of soil moisture: a hydrologic perspective. *Annu. Rev. Earth Planet. Sci.* 30, 149–180. <https://doi.org/10.1146/annurev.earth.30.091201.140434>.
- Wood, E.F., Roundy, J.K., Troy, T.J., van Beek, L.P.H., Bierkens, M.F.P., Blyth, E., de Roo, A., Döll, P., Ek, M., Famiglietti, J., Gochis, D., van de Giesen, N., Houser, P., Jaffé, P.R., Kollet, S., Lehner, B., Lettenmaier, D.P., Peters-Lidard, C., Sivapalan, M., Sheffield, J., Wade, A., Whitehead, P., 2011. Hyperresolution global land surface modeling: meeting a grand challenge for monitoring Earth's terrestrial water. *Water Resour. Res.* 47. <https://doi.org/10.1029/2010wr010090>.
- Zhan, X., Houser, P.R., Walker, J.P., Crow, W.T., 2006. A method for retrieving high-resolution surface soil moisture from hydro L-band radiometer and radar observations. *IEEE Trans. Geosci. Remote Sens.* 44 (6), 1534–1544.
- Zhao, Y., Vergopolan, N., Baylis, K., Blekking, J., Caylor, K., Evans, T., Giroux, S., Sheffield, J., Estes, L., 2018. Comparing empirical and survey-based yield forecasts in a dryland agro-ecosystem. *Agric. For. Meteorol.* 262, 147–156. <https://doi.org/10.1016/j.agrformet.2018.06.024>.